Charles University in Prague

Faculty of Science

Chemistry

Physical Chemistry

Lucie Suchá

Interaction of Branched Copolymers with Low Molar Compounds – Dissipative Particle Dynamic Study

Interakce větvených kopolymerů s nízkomolekulárními sloučeninami – studie pomocí disipativní částicové dynamiky

Diploma Thesis

doc. Ing. Zuzana Limpouchová, CSc.

Prague, 2015

Prohlášení

Prohlašuji, že jsem závěrečnou práci zpracovala samostatně a že jsem uvedla všechny použité informační zdroje a literaturu. Tato práce ani její podstatná část nebyla předložena k získání jiného nebo stejného akademického titulu.

V Praze, 11. 05. 2015

Lucie Suchá

Acknowledgements

This research was funded by Grant 328514 of the Grant Agency of the Charles University and by Czech Science Foundation Grant P106-12-0143 and 13-02938S. Computational resources were provided by the MetaCentrum under the program LM2010005 and the CERIT-SC under the program *Centre CERIT Scientific Cloud*, part of the *Operational Program Research and Development for Innovations*, Reg. no. CZ.1.05/3.2.00/08.0144.

First and foremost, I would like to thank my research supervisor, doc. Ing. Zuzana Limpouchová, CSc., and prof. RNDr. Karel Procházka DrSc., for their patience, advices and their valuable experiences.

I would also like to thank to whole members of the Soft Matter group for sharing the experiences and nice study atmosphere.

The greatest thanks go to my friends (especially Mr Amundsen), who are responsible for my sanity even after all the years of study.

Contents

Abstrakt

Tato diplomová práce se věnuje studiu počítačových simulací interakcí blokových amfifilních kopolymerních dendrimerů v roztocích pomocí částicové disipativní dynamiky (DPD). Největší pozornost je věnována solubilizaci nízkomolekulárních látek do solvofobní části dendrimeru. Studované dendrimery mají dvě vnitřní solvofobní patra a jedno nebo dvě vnější solvofilní patra. Solubilizovanou látkou je buď solvofobní monomer, nebo tetramer.

Úvodní část práce obsahuje základní informace o dendrimerech a popis simulační metody včetně použitých veličin.

Druhá část práce je věnována výsledkům simulací solubilizace nízkomolekulární solvofobní látky do kopolymerního dendrimeru. Jsou v ní diskutovány a analyzovány nejdůležitější trendy chování velikosti a vnitřní struktury agregátů. Bylo zjištěno, že pro solubilizaci dostatečně velkého množství nízkomolekulární látky je nezbytné, aby byla solvofobní látka do dendrimerního jádra »přitahována«, tj. aby se rozpouštěla přednostně v jádře dendrimeru. Solubilizace nízkomolekulární látky byla studována v závislosti na síle přitažlivé interakce a koncentraci monomeru, respektive tetrameru, a v závislosti na architektuře a složení kopolymerního dendrimeru

Závěrem lze říci, že nejslibnější systémy pro aplikaci jsou ty s relativně dlouhým lineárním úsekem mezi větvícími body a dostatečným množstvím dostatečně dlouhých vnějších solvofilních pater. Vhodné jsou solvofobní látky, které jsou v dendrimerním jádře velmi dobře rozpustné. Taktéž použití oligomerních řetězců má příznivý vliv na jejich solubilizaci.

Klíčová slova: Disipativní částicová dynamika, počítačové simulace, amfifilní, kopolymery, dendrimery, selektivní rozpouštědlo, solubilizace, konformační chování

Abstract

The presented diploma thesis is devoted to computer simulations of the interactions of amphiphilic copolymer dendrimers in diluted solutions by means of the dissipative particle dynamics. We focus mainly on the solubilization of low molar compounds in the solvophobic part of dendrimer in selective solvents. Studied copolymer dendrimers have two inner solvophobic generations and one or two outer solvophilic generations. The solubilized compounds are solvophopic monomer and tetramers.

In the first part of the diploma thesis, fundamental information about dendrimers is presented and the principles of the applied simulation methods are explained together with the definition of used quantities.

The second part is devoted to the study of solvophobic low molar compound solubilization in the copolymer dendrimer. The most important trends concerning the size and inner structure of aggregates are analysed and discussed. We have found that the preferential attraction between solvophobic compound and solvophobic dendrimer core is essential for a sufficient solubilization. The solubilization of low molar compound was studied as function of the attractive interaction and concentration of monomers, resp. tetramers, and the copolymer dendrimer architecture and composition.

We conclude that the most prospective systems from the application point of view are dendrimers with relatively long spacer and large enough outer solvophilic shell. The solvophobic compounds with the attraction to the dendrimer core are more proper than the compounds without the attraction. Simultaneously the oligomer chains promote the solubilization.

Keywords: Dissipative particle dynamics, computer simulations, amphiphilic, copolymers, dendrimers, selective solvent, solubilization, conformational behavior

List of symbols and abbreviations

a	repulsion parameter
A_g	aggregation number
A_i	pre-exponential factor for autocorrelation function
c	total bead concentration
c_0	reference concentration
f	connectivity of the branching point
f_C	connectivity of the central core
$F_n(A_g)$	number distribution function of aggregation numbers
$F_w(A_g)$	weight distribution function of aggregation numbers
$\vec{F}_i$	force acting on a particle
$\vec{F}_{ij}^C$	conservative force
$\vec{F}_{ij}^D$	dissipative force
$\vec{F}_{ij}^R$	random force
$\vec{F}_{i,i+1}^S$	spring force between adjacent particles
g	number of dendrimer generations
k_B	Boltzmann's constant
k_S	spring constant
L	simulation box edge length
m_i	mass of ith particle
m_{A_g}	mass of an aggregate with aggregation number A_g
n	number density of molecules
N	number of particles in system
$N(A_g)$	number of associates consisting of A_g monomers
$N(r)$	number of beads in spherical layer
$\mathcal{N}$	number of beads in polymer chain
p	pressure
r	radius of spherical layer
r_0	equilibrium distance
r_c	cutoff radius
r_{ij}	distance between ith and jth particle

$\vec{r}_i$	position vector of the ith particle
$\vec{r}_{ij}$	vector connecting ith and jth particle
$\hat{r}_{ij}$	unit vector in the direction $\vec{r}_{ij}$
$\vec{R}$	position vector of the center of mass
R_g	gyration radius
$R_g(\mathrm{A}_1)$	gyration radius of the solvophobic part of dendrimer
s	length of spacer
t	time
T	temperature
$\vec{v}_i$	velocity vector of the ith particle
$\vec{v}_{ij}$	relative velocity between ith and jth particle
V	volume of the system
$V(r)$	volume of spherical layer
$w^D(r_{ij})$	weight function for dissipative force
$w^R(r_{ij})$	weight function for random force
X	arbitrary quantity
α	empiric constant of the equation of state
γ_{ij}	drag coefficient
Δa	excess repulsion
Δi	time step interval
Δt	time step
ζ_{ij}	random variable with Gaussian distribution
κ^{-1}	compressibility
ρ	particle number density
$\rho(r)$	radial number density of beads
σ_{ij}	noise amplitude
τ	autocorrelation time
χ	Flory-Huggins parameter

ACF	autocorrelation function
A_1	solvophobic dendrimer beads
A_2	solvophilic dendrimer beads
B	beads of solvophobic monomer, resp. tetramer
DPD	dissipative particle dynamics
MD	molecular dynamics
S	beads of solvent

1 Introduction

Polymers play important role in human life. The naturally occurring polymers have been used by humankind for ages without realizing that these substances are macromolecules. At the beginning of the 20th century, the scientists proposed the hypothesis that polymers are large molecules formed of a high number of covalently bonded units, called the monomer units (derived from monomers; the monomer unit is not always identical with the repeating unit, which represent the shortest repeating part of the chain). Shortly afterwards, the first attempts to synthesize polymers were successfully accomplished, their covalent structure was unambiguously proven and since then various advanced synthetic (polymerization) have been developed and optimized.

Nowadays, the polymers can be found in all spheres of activities of the human society – typical synthetic polymer products span form everyday consumables (plastic bags, containers, clothes, parts of various tools, etc.) to the most advanced technologies and nanotechnologies in medicine or optoelectronic. Besides synthetic polymers produced in tons in chemical plants all over the world, the biopolymers are omnipresent biologically important building materials of plants, and vital constituents of animal and human bodies (proteins, polysaccharides, nucleic acids, etc.).

Polymer is a large molecule consisting of one or several types of repeating units that are connected to each other in long linear sequences by covalent bonds and form macromolecules of various architectures (e.g., linear, branched, crosslinked, etc. see Fig. 1.1). The chemical and physical properties of polymers depend on the nature of building units, type and strength of interconnecting bonds, composition, molecular weight (degree of polymerization) and on the chain architecture, i.e., on the way how the units are connected to each other.

Depending on the chemical composition, the polymers can be divided into two basic classes: (i) homopolymers, composed of one type of building unit and (ii) copolymers, which contain two or more monomer units. The interconnection of bifunctional monomers or monomers with one reactive double bond leads to liner chains, while the copolymerization with a low fraction of multifunctional species results in branched or crosslinked polymers. Various tailored structures (hyperbranched, star-like, comb-like or polymer dendrimes, etc.) can also be prepared by advanced

targeted polymerization techniques. [1]

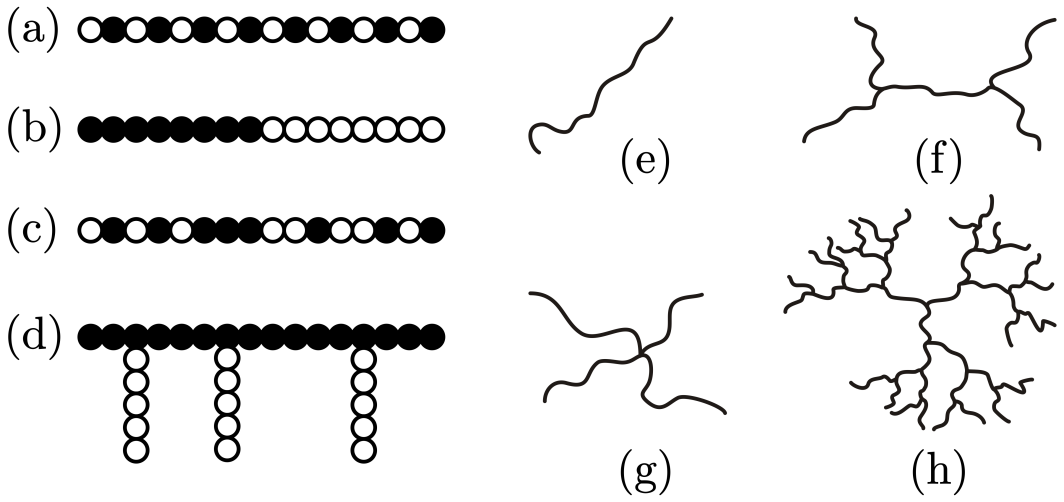

Figure 1.1: Examples of different copolymer types: (a) alternating, (b) block, (c) statistical (or random), (d) graft copolymer; and the different polymer architecture: (e) linear, (f) H-branched, (g) star-branched, (h) dendritic polymer chain.

This diploma thesis concerns the computer study of the behavior of polymer dendrimers and their interaction with other molecules in dilute solutions. At present, computer simulations play very important role in macromolecular science. They facilitate the interpretation of experimental results, reveal detailed pieces of information which are often inaccessible to experimental studies, predict new phenomena and their results can be used for optimization of experimental studies.

Computer simulations can be also used as *pseudo-experimental* methods for testing predictions of analytical theories, which in addition to somewhat simplified description of interactions often employ other simplifying assumptions and various mathematical approximations. If the forces are described by the same formulas in both types of methods, the differences between theoretical predictions and simulations results quantify the effect of simplifications used in the theoretical treatment.

Accurate computer simulations of complex systems are very time- and computer memory-demanding and require the use of very powerful computers. Thanks to recent advances in computer technology, relatively large and complex system can be reliably studied by simulations, but the study of polymer systems on the atomistic level (when the interactions between all individual atoms are taken into account) exceeds the capabilities of the most powerful up-to-date supercomputers and is abso-

lutely impossible. The fine coarse-grained methods (where the interaction between monomer units is approximately described by, e.g., the Lennard-Jones potentials and the chains are represented by the *"bead-spring"* models) can be efficiently used in studies of single chains (usually in implicit solvent). The investigation of properties of polymer and polyelectrolyte solutions and studies of polymer self-assembly usually require the use of rough coarse-grained methods, such as the dissipative particle dynamics (DPD). This method has been employed in the thesis for studying the interaction of amphiphilic polymer dendrimers with other molecules (solvophobic monomers and oligomers) and its principle and obtained results will be described and discussed in next parts of the thesis. [2, 3]

2 Aims of the thesis

The DPD simulations, presented in this thesis, are aimed at the enhancement of solubility of solvophobic compounds based on their interaction of with amphiphilic dendrimers. They should contribute to the understanding of solubilization of low molar mass compounds and oligomers in copolymer dendrimers and elucidate how the solubilization capacity depends on the interaction parameters, composition and architecture of dendrimers.

3 Dendrimers

This work deals with one subclass of hyperbranched polymers - dendrimers. The term *dendrimer* derives from the two ancient Greek words *dendra* = tree and *meros* = part. These highly branched monodisperse macromolecules (the monodispersity can be verified by experimental methods such as high performance liquid chromatography or size exlusion chromatography) exhibit regular globular structure in nanometre size with large number of peripheral groups. Properties of dendrimers (e.g., solubility, viscosity, diffusivity) differ significantly from those of linear polymers of a similar molecular weight. Dendrimers are application-attractive species due to their specific and unique features. They are promising candidates for additives, chemical catalysts, stimuli sensitive molecules, macromolecular building blocks or nanocontainers etc. [4, 5, 6, 7]

Dendrimers are characterized by the number of generation, g, which refers to the number of linear parts between central core and arbitrary free end, the number of monomers in the chain between two branching points called spacer, s, connectivity of the central core and the branching points, f_C and f, as is shown in Fig. 3.1. [5]

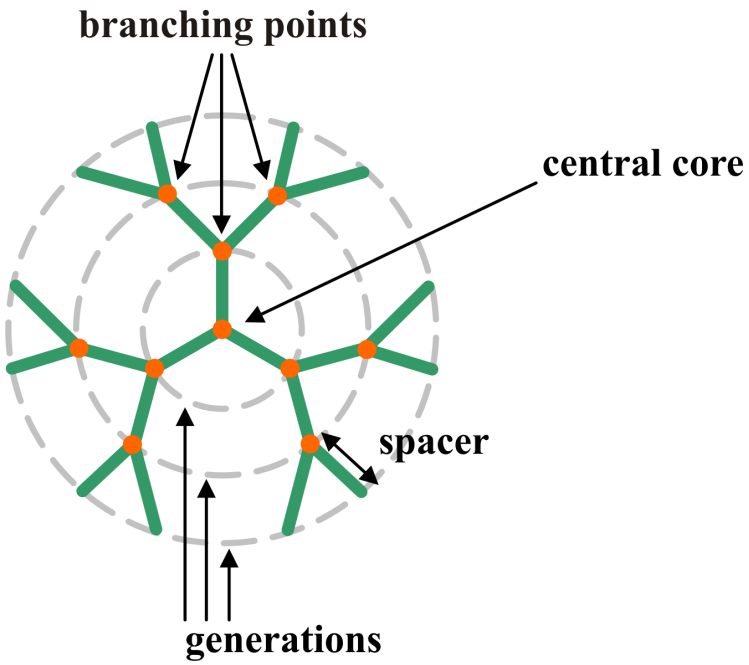

Figure 3.1: Schematic representation of the three-generations-dendrimer with $f_C = f = 3$.

The branched (dendritic) architecture is one of the most often observed topology

in the biological systems – it can be found from the meter scale (e.g., tree branching, roots) to micrometer scale (e.g., neurons). Also other types of polymers show this architecture. Some examples are depicted in Fig. 3.2. [6]

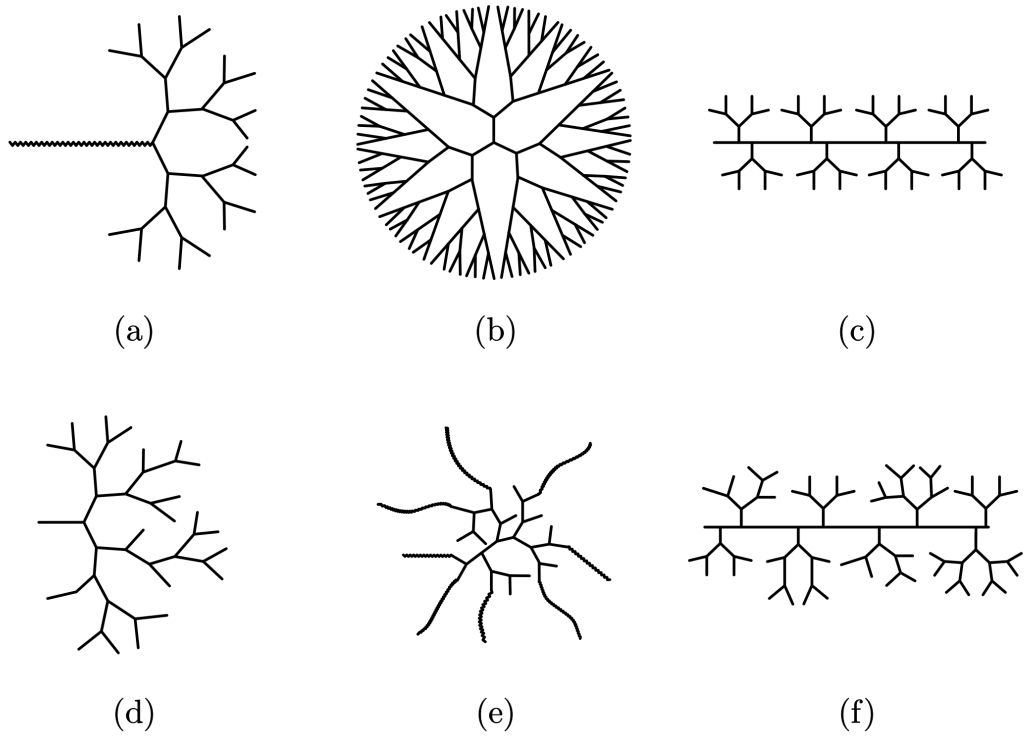

Figure 3.2: Examples of dendritic architecture: (a) linear dendritic hybrid, (b) dendrimer, (c) dendronized (or dendrigrafted), (d) hyperbranched, (e) multiarm star, (f) hypergrafted polymer.

3.1 Dendrimers as nanoscale containers

Dendrimers are, because of their architecture and properties, attractive for a number of different applications including drug delivery. They may encapsulate drugs in their hydrophobic dendrimer interior, which is well-suited for the guest-host interaction, while the hydrophilic exterior secures their solubility. This effect can be used in pharmacy, because most of drugs are hydrophobic and poorly soluble. The encapsulation can be influenced by many factors, e.g., dendrimer generation size, concentration, pH of solution, etc.

Furthermore dendrimers show topologies and behavior reminiscent of polymer micelles. Dendrimers with apolar core and polar shell create unimolecular micelles,

thus, in contrast with polymer micelles, it isn't necessary to reach critical micelle concentration. [8, 9, 10]

3.2 Conformational behavior of polymer dendrimers

Polymer dendrimer configuration is determined by the balance between the repulsive excluded volume interaction, the repulsive solvophobic or attractive solvophilic interactions with solvent and the entropic penalty due to the spacers conformation (usually expansion due to the excluded volume interaction).

Several simulation methods (mean-field [12, 13], Monte Carlo [14, 15], molecular dynamics [16] and also scaling approach [17]) proved that the density of neutral homopolymer dendrimer is greatest at the core of polymer dendrimer. The density profile dependence on the radial distance from the core has the same shape at all solvent conditions: small local minimum between the central maximum and the plateau region and the relatively slow decrease at the periphery of the dendrimer. Simultaneously it was showed that the terminal groups are not fixed on the surface of a dendrimer, but are distributed through the whole dendrimer volume.

Further, the segregation of individual branches (dendrons) was proved for homogeneous dendrimers [18] as well as for so called codendrimers that are formed from chemically different dendrons. [20]

It follows from the segment densities that the amphiphilic copolymer dendrimers are more promising from the application point of view, as the typical applications of polymer dendrimers assume a space inside the core, which can be used for selective solubilization of solvophobic compounds from the solution in the dendrimer core.

The computer simulations are very useful tool for preliminary evaluation of copolymer dendrimer structures. The internal structure of copolymer dendrimer can be controlled, e.g., by the use of amphiphilic copolymers with the inner and outer generations differing in the length and the flexibility of spacers or in the interaction parameters or by the use of stimuli responsive polyelectrolytes. [21, 22]

The internal structure of copolymer dendrimer can be also controlled by the chemical composition of dendrimer, e.g., polymer dendrimers with short rigid inner generations and with flexible long outer generation or with inner solvophobic generations protected by solvophilic outer generations can be used. The functional dendrimers modified by with specific groups at the end of arms or at the branching

points were also studied. [23, 24]

Recently, computer simulations of dendrimer were summarized in two reviews. [25, 26]

3.3 Complexation of neutral copolymer dendrimers with solvophobic compounds

The research on interaction of copolymer dendrimers with solvophobic compounds in solution is important task from the application point of view, so a number of theoretical and simulation studies have been devoted to the individual systems. A lot of them were summarized in two recent comprehensive review focused particularly on targeted delivery systems. [27, 28]

Almost all of these studies deal with polyelectrolyte dendrimers in aqueous solutions. The interaction of neutral copolymer dendrimers with solvophobic compounds in selective solvents was studied relatively rarely despite the fact that such model system (without electrostatic interaction) enables to elucidate the effect of the copolymer and solute architectures and the interplay of the solvophobic and solvophilic interactions among individual parts of copolymer dendrimer, solvophobic solute and solvent.

Up to our knowledge only one similar study to our work was published. [29] The authors also used the dissipative particle dynamics, however their study is rather preliminary without careful equilibration and with rather unrealistic interaction parameters.

4 Dissipative particle dynamics

Dissipative particle dynamics (DPD) has been chosen as the simulation method. It is an off-lattice, coarse-grained method that conserve momentum. The DPD is useful for simulating systems on the near-molecular scale such as polymers, biopolymers, lipids, emulsions and surfactants.

This technique has been introduced by Hoogerbrugge and Koelman in the 1990s as a novel method for simulating hydrodynamic phenomena, based on the combination of Molecular Dynamics (particularly Brownian Dynamic) and Lattice-Gas Automata. [30]

DPD similarly to Molecular Dynamics (MD) preserve the momentum (and thus hydrodynamic behavior), but DPD allows to simulate behavior on larger length and time scales than MD, because DPD particles (usually called *beads*) do not represented individual atoms but they are a coarse-grained representations of parts of large molecules (e.g., functional groups), whole molecules or fluid regions (see Fig. 4.1). These spherical beads interact with each other via soft forces and can mutually interpenetrate relatively easily.

Numerical solutions of the equations of motion is easier than for MD, for two reasons: (i) in MD, the equations are solved for each particle (even the solvent), (ii) in DPD the forces are soft and do not diverge and therefore longer time-steps can be used. [3, 31, 32, 33, 34, 35]

The time evolution of particles in the system is governed by Newton's equations of motion:

$$\frac{d\vec{r}_i}{dt} = \vec{v}_i \tag{4.1}$$

$$\frac{d\vec{v}_i}{dt} = \frac{\vec{F}_i}{m_i}, \tag{4.2}$$

in which t stands for time, m_i is mass of ith particle with position vector $\vec{r}_i$, velocity vector $\vec{v}_i$ and force vector $\vec{F}_i$, represents all forces acting on a particle and is a sum of a three pair forces:

$$\vec{F}_i = \sum_{j \neq i} (\vec{F}_{ij}^C + \vec{F}_{ij}^D + \vec{F}_{ij}^R) \tag{4.3}$$

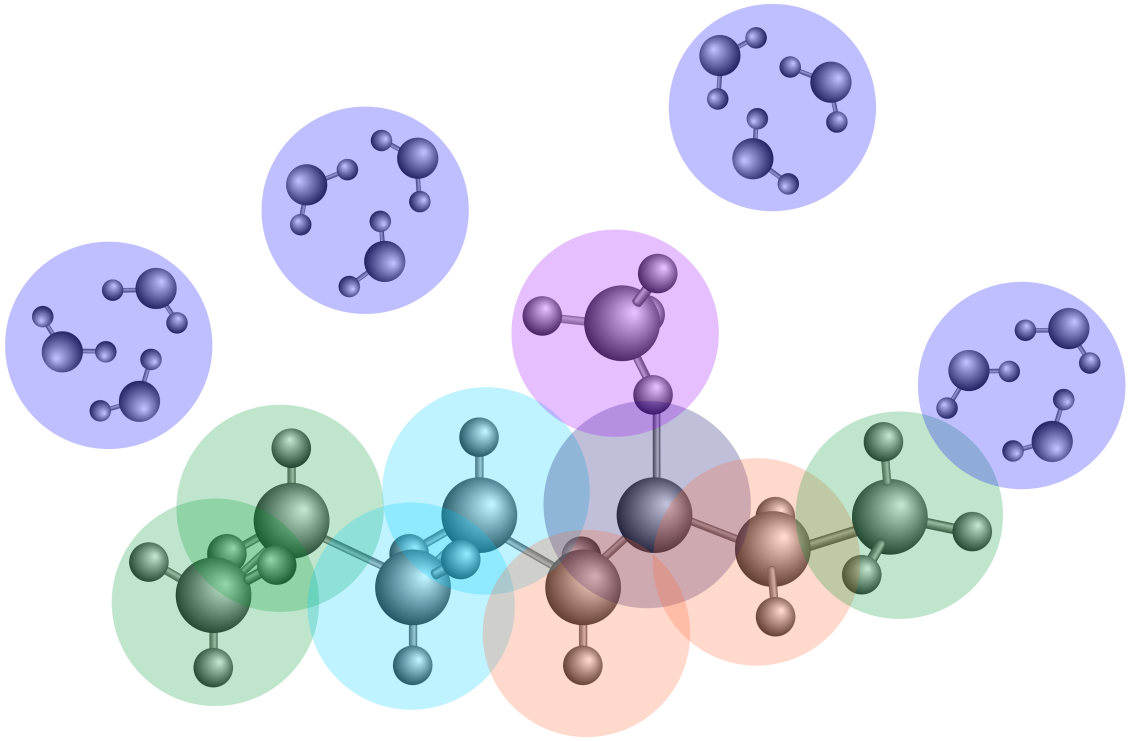

Figure 4.1: Coarse-grained DPD particles – *beads* can represent whole molecules or fluid regions.

where $\vec{F}_{ij}^{C}$, $\vec{F}_{ij}^{D}$ and $\vec{F}_{ij}^{R}$ are the conservative, dissipative (or drag) and random (or stochastic) pair forces.

The conservative force is a *soft* (i.e., weakly interacting) repulsing force and is given by:

$$\vec{F}_{ij}^{C} = \begin{cases} a_{ij}(1 - \frac{r_{ij}}{r_c})\hat{r}_{ij} & \text{for } r_{ij} < r_c, \\ 0 & \text{for } r_{ij} \geq r_c, \end{cases} \tag{4.4}$$

where a_{ij} is a maximum repulsion between particle i and j (may be the same for all particle pairs or may be different for different particle types), r_{ij} is their distance which is given by $r_{ij} = |\vec{r}_{ij}| = |\vec{r}_i - \vec{r}_j|$ and $\hat{r}_{ij}$ is normalized vector $\vec{r}_{ij}$ ($\hat{r}_{ij} = \frac{\vec{r}_{ij}}{r_{ij}}$). The r_c is cutoff radius which describes the range of forces.

The dissipative force $\vec{F}^{D}$ corresponds to the frictional force which depends both on the relative velocities and the positions between interacting pairs of particles.

$$\vec{F}_{ij}^{D} = -\gamma_{ij} w^{D}(r_{ij}) \cdot (\hat{r}_{ij} \cdot \vec{v}_{ij})\hat{r}_{ij}, \tag{4.5}$$

where the constant γ_{ij} is the drag coefficient, w^{D} is a weight function and $\vec{v}_{ij}$ denotes a relative velocity which is given by $\vec{v}_{ij} = \vec{v}_i - \vec{v}_j$.

The random force has the form:

$$\vec{F_{ij}^R} = \sigma_{ij} w^R(r_{ij}) \zeta_{ij} \frac{\hat{r}_{ij}}{\sqrt{\Delta t}}, \tag{4.6}$$

where constant σ_{ij} is a noise amplitude and is related to the temperature, as is understood from the role of the stochastic force in representing a heat bath, w^R is a weight function, Δt is the time step and ζ_{ij} is a random variable with Gaussian distribution with zero mean and unit variance chosen independently for each pair of interacting particles and each time step and $\zeta_{ij} = \zeta_{ji}$ (this symmetry ensures that the total momentum is conserved). The random force represents random collisions between particles.

The r-dependent weight functions w^D and w^R in equations (4.5) and (4.6) can not be chosen arbitrarily. Español and Warren in [35] showed that the simulations conserve energy only if the fluctuation-dissipation theorem is fulfilled, i.e., only if the following relations are satisfied:

$$w^D(r_{ij}) = [w^R(r_{ij})]^2 \tag{4.7}$$

$$\sigma_{ij}^2 = 2\gamma_{ij} k_B T, \tag{4.8}$$

where k_B denotes Boltzmann's constant and T is temperature. In practice, the weight functions are typically defined through:

$$w^D(r_{ij}) = \left[w^R(r_{ij})\right]^2 = \begin{cases} (1 - \frac{r_{ij}}{r_c})^2 & \text{for } r_{ij} < r_c, \\ 0 & \text{for } r_{ij} \geq r_c. \end{cases} \tag{4.9}$$

The dissipative and random forces also act as a thermostat.

The polymer chain in DPD is modeled as a string of beads i and $i+1$ connected by springs. For this purpose, linear harmonic spring is used:

$$\vec{F}_{i,i+1}^S = -k_S(r_{i,i+1} - r_0)\hat{r}_{i,i+1}, \tag{4.10}$$

where $\vec{F}_{i,i+1}^S$ denotes elastic force, k_S spring constant and r_0 is an equilibrium distance between two particles, which is often set to 0, because particles can theoretically pass through each other freely, but the finite bond length are assured by repulsive force.

The algorithm for integration of the equations of motion (4.1) and (4.2) is based

on the second-order velocity-Verlet scheme:

$$\begin{aligned}
\vec{v_i}(t+\frac{1}{2}\Delta t) &= \vec{v_i}(t) + \frac{\vec{F_i}(t)}{2m}\Delta t, \\
\vec{r_i}(t+\Delta t) &= \vec{r_i}(t) + \vec{v_i}(t+\frac{1}{2}\Delta t)\Delta t, \\
\vec{F_i}(t+\Delta t) &= \vec{F_i}(\vec{r_i}(t+\Delta t), \vec{v_i}(t+\frac{1}{2}\Delta t)), \\
\vec{v_i}(t+\Delta t) &= \vec{v_i}(t+\frac{1}{2}\Delta t) + \frac{\vec{F_i}(t+\Delta t)}{2m}\Delta t.
\end{aligned} \tag{4.11}$$

4.1 System of units

In simulation, it is often suitable to express the used quantities in reduced units (or non-dimensional units), because SI units are for simulations either too large or too small. The unit of the length is the cutoff radius r_c, energy is measured in units of k_BT and the unit of mass is mass of one particle m_i. [3, 31]

In the following text, the quantities in reduced units will be marked by asterisk(*), thus the reduced distance $r^* = \frac{r}{r_c}$, the reduced repulsion parameter $a^*_{ij} = \frac{a_{ij}r_c}{k_BT}$ and the reduced time $t^* = r_c\sqrt{\frac{m}{k_BT}}$. [32]

4.2 Parametrization of DPD

Because DPD employes only repulsive forces, the condensed system (liquid) is kept together by external pressure. The equation for pressure, obtained from the virial theorem, has a form:

$$p = \rho k_B T + \frac{1}{3V}\left\langle \sum_{j>i} (\vec{r_i} - \vec{r_j}) \cdot \vec{F_i} \right\rangle, \tag{4.12}$$

where p denotes pressure, ρ is the particle number density and V denotes volume of the system. Force $\vec{F_i}$ can be according to [31] identified with conservative force $\vec{F}^C_{ij}$.

Groot and Waren [31] shown through a series of equilibrium simulations with different values of conservative force coefficient a^*_{ij} and density, that for sufficiently large densities ($\rho^* > 2$) the equation for pressure can be well-approximated by the equation of state:

$$p^* = \rho^* + \alpha^* a^* \left(\rho^*\right)^2 \qquad \alpha^* = 0.101 \pm 0.001, \tag{4.13}$$

where α^* is an empiric constant the equation of state and density ρ^* is expressed as $\rho^* = \rho r_c^3 = \frac{N^*}{V^*}$, where $N^* = N$ is total number of particles and $V^* = \frac{V}{r_c^3}$.

The dimensionless isothermal compressibility can be defined as:

$$\kappa^{-1} = \frac{1}{k_B T} \left(\frac{\partial p}{\partial n} \right)_T \tag{4.14}$$

where n is the number density of molecules. Combining the known compressibility of water ($\kappa^{-1} \sim 16$ for $T = 300$ K) with the compressibility which can be obtained from (4.14), they derived the following formula for the repulsive parameter a^*:

$$a^*_{ii} = \frac{75}{\rho^*} \tag{4.15}$$

They have shown that $\rho^* = 3$ is a reasonable choice for the particle density, therefore $a^*_{ii} = 25$ is usually used.

Groot and Waren [31] also mapped the repulsion parameter a^*_{ij} (the repulsion parameter for different particles) onto the Flory-Huggins theory. They found the relationship between a^*_{ij} and the Flory-Huggins parameter χ_{ij} as:

$$\chi_{ij} = 2\alpha^*(a^*_{ij} - a^*_{ii})(\rho^*_i + \rho^*_j), \tag{4.16}$$

where $(\rho^*_i + \rho^*_j) = \rho^*$. Under the assumption $a^*_{ii} = a^*_{jj}$, the formulas (4.15) and (4.5) have for $\rho^* = 3$ the form:

$$a^*_{ij} = a^*_{ii} + \Delta a^* = 25 + 3.27\chi_{ij}, \tag{4.17}$$

where $\Delta a^* = a^*_{ij} - a^*_{ii}$ is the excess repulsion.

5 Simulations

5.1 Used software

All simulations were performed using the simulation software DL_MESO. This software is a parallel mesoscale simulation package containing dissipative particle dynamics and the lattice Boltzmann equation method and is issued free under licence to academic institutions pursuing scientific research of a non-commercial nature (see [33, 34] for more details).

My own software written in C++ has been used for generating the input data and for the post processing of the obtained simulations data.

5.2 Studied system

In this work, the solubility properties of copolymer dendrimers were studied in infinitely diluted solutions in selective solvents. In the following text only reduced units are used, so the asterisk is omitted.

Solvent will be denoted by symbol S. The studied dendrimers contain two distinct incompatible parts − inner solvophobic part, A_1, and outer solvophilic shell, A_2. Unless otherwise stated, the simulation box contains also the low molar compound (denoted by B), which can be solubilized in to the solvophobic core of the dendrimers. Low molar compound was modeled as one bead (monomer) or four beads binded together (tetramer).

The changes of dendrimer size and changes of internal structure due to the solubilization of solvophobic compounds in the dendrimer were monitored and the effects of (i) solvent selectivity, (ii) total bead concentration of solvophobic compound, (iii) its size (monomer or tetramer) and (iv) number generation were systematically studied.

5.2.1 System parameters

The dendrimers with three generation (respectively with four generation) with two solvophobic inner blocks (A_1 type) and one (resp. two) peripheral solvophilic block (A_2 type) were studied, because they are expected to secure efficient solubilization of solvophobic compounds and they are more biocompatible than dendrimers with

the higher number of generations. [9] The connectivity of the central core and the branching points were the same - $f_C = f = 3$. The spacer length was the same for all generation, $s = 5$ or $s = 7$.

The behavior of infinitely diluted polymer solution was studied, i.e., only one dendrimer was present in the simulation box. The cubic simulation box with periodic boundary conditions was used. The box size was $L = 22$ for the spacer $s = 5$ and $L = 30$ for the spacer length $s = 7$.

All simulations were performed with the time step $\Delta t = 0.05$, noise amplitude $\sigma_{ij} = 3.0$ and thus (according to eq. (4.8)) with the friction coefficient $\gamma = 4.5$ in cubic simulation box with the particle density $\rho = 3$. Polymer chain has been modeled using the harmonic spring potential (see eq. (4.10)) with parameters $r_0 = 0$ and $k_S = 4$. The cutoff radius r_c and bead mass m were set to 1 (which is consistent with the reduced units).

The total bead concentration of solvophobic monomer was variable. For a smooth discussion, the concentration $\frac{1}{270}N \approx 3.7 \cdot 10^{-3}N$ was defined as the reference concentration c_0. The reference concentration corresponds to 118 solvophobic monomers for dendrimer with spacer 5 (in box with $L = 22$) and 300 monomers for dendrimer with $s = 7$ (in box with $L = 30$). The total bead concentrations of solvophobic monomer compound were changing from 0 to $6.0c_0$.

The length of simulation runs was chosen with respect to autocorrelation time. Every $(\tau/2)$th configuration was saved for better statistic. The total number of saved configuration of equilibrated system was 2500.

The strength of interactions between beads is described by the repulsion parameter a. For a clear (and non-confusing) discussion of obtained results, it is necessary to realize that the attraction in DPD method is (similarly to the commonly used Flory-Huggins theory of concentrated solutions [1]) described as a weaker repulsion between corresponding beads in comparison with the repulsion between other types of bead pairs. Thus a value lesser than 25 implies that two beads are attracted.

Two different sets of repulsion parameters were used to study interaction between dendrimer and solvophobic compound.

The first set of simulations were performed with only two different parameter values: one for favourably interacting bead pairs $a = 25$ and the second for pairs of unfavourably interacting beads $a = 50$, 47, 45 and 40.

The second set of repulsion parameters contained three different values. The repulsive interaction between pairs of unfavourably interacting beads is described by $a = 40$. The solubilization of solvophobic compound in the dendrimer core is supported by repulsion parameter $a_{(\mathrm{B}|\mathrm{A}_1)} = 20$, 22.5 or 25. The repulsion parameter 25 is introduced to make a bridge between these two parameters sets.

In both cases the repulsion parameter between the same species a_{ii} was set as 25 and all values of repulsion parameters are summarized in tab. 5.1. and tab. 5.2.

	S	B	A_1	A_2
S	25	a	a	25
B		25	25	a
A_1			25	a
A_2				25

Table 5.1: Values of the repulsion parameter in two parameters study. The changing parameter $a = a_{(\mathrm{S}|\mathrm{B})} = a_{(\mathrm{S}|\mathrm{A}_1)} = a_{(\mathrm{B}|\mathrm{A}_2)} = a_{(\mathrm{A}_1|\mathrm{A}_2)}$ describes repulsive interaction between pairs of unfavorably interacting beads.

	S	B	A_1	A_2
S	25	40	40	25
B		25	a	40
A_1			25	40
A_2				25

Table 5.2: Values of the repulsion parameter in three-parameters-study. The changing parameter $a = a_{(\mathrm{B}|\mathrm{A}_1)}$ describes attractive interaction between solvophobic compound and solvophobic part of dendrimer

In the case of using different sets of repulsion parameters, they are specify for that given case.

5.3 Analyzed physical quantities

For the analysis of simulation results and for the description of the solubilization of the solvophobic compound in the dendrimer core, the following physical quantities were used:

5.3.1 Gyration radius

The gyration radius R_g gives information on the size of the dendrimer. Its square R_g^2 for polymer with $\mathcal{N}$ beads is defined as:

$$R_g^2 = \frac{1}{\mathcal{N}} \sum_{i=1}^{\mathcal{N}} (\vec{r}_i - \vec{R})^2, \tag{5.1}$$

thus describes the mean square of average squared distance between beads of polymer in given conformation $\vec{r}_i$ and the polymers center of mass (represent by $\vec{R}$). [1]

The gyration radius of the whole dendrimer was monitored. The experimental measurement of dendrimer size in terms of Rg can be performed by light scattering. [36]

The gyration radius of the inner solvophobic part of the dendrimer was also evaluated. This quantity reflects the change in the core size due to the process of solubilization of solvophobic monomer, resp. tetramer.

5.3.2 Autocorrelation function

The consecutive states of the simulated system are correlated because only a small change of beads velocities and coordinates occurs during one simulation step. For the evaluation of statistically meaningful data, it is crucial to use the uncorrelated states. Therefore the autocorrelation (or relaxation) time τ, which represents the number of steps between two uncorrelated states, has to be evaluated. The autocorrelation function (ACF) of arbitrary quantity X as a function of a time t can be calculated as:

$$\mathrm{ACF}(t) = \frac{\langle X_s X_{s+t} \rangle - \langle X_s \rangle^2}{\langle X_s^2 \rangle - \langle X_s \rangle^2}, \tag{5.2}$$

where $\langle X \rangle$ is mean of X, $\langle X^2 \rangle$ is its mean square, $\langle X_s^2 \rangle - \langle X_s \rangle^2$ has the meaning of the variance and $\langle X_s X_{s+t} \rangle = \frac{1}{K-t} \sum_{1}^{K-t} X_s X_{s+t}$.

It can be shown that the ACF usually decreases as an exponential function or as a sum of exponential functions, i.e., $\mathrm{ACF}(t) \sim \sum_j A_j \exp(-\frac{t}{\tau_j})$ and ACF can be fitted by exponential curve in this form.

To find the number of steps between two uncorrelated states, the simulation runs were performed with a very short time step interval ($\Delta i = 10$) between the accounted configurations and autocorrelation functions were evaluated. Because of

focusing on the changes in dendrimer size due to the solubilization, the ACF was based on the distance between the center of mass and the 2nd branching points.

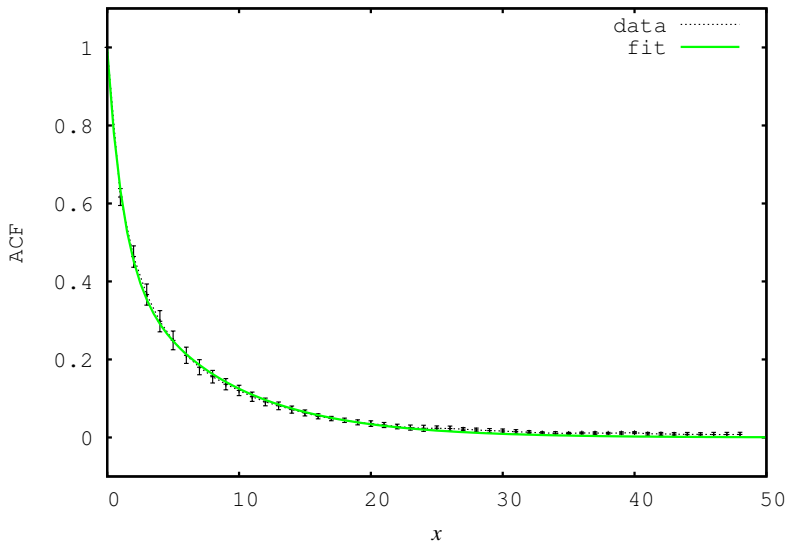

Figure 5.1: The example of autocorrelation function of distance between center of mass and the 2nd branching points of dedrimer with $s = 5$, $g = 3$ and $a_{(\mathrm{B}|\mathrm{A}_1)} = 20$ in solvent with solvophobic monomer($c = c_0$).

5.3.3 Radial number density of beads

The radial number density of beads $\rho(r)$ is defined as the ratio of the number of beads of a given type in spherical layer around the dendrimer center of mass, $N(r)$, to the volume of this layer $V(r)$:

$$\rho(r) = \frac{N(r)}{V(r)}, \tag{5.3}$$

$$V(r) = \frac{4}{3}\pi\left((r + \Delta r)^3 - r^3\right), \tag{5.4}$$

where r is inner radius of the layer and Δr is layer width.

The radial number density of polymer beads describes the dendrimer compactness and the radial number bead density of solvophobic monomer (tetramer) and solvent beads characterizes their incorporation in the dendrimer.

5.3.4 Aggregation number

The aggregation (or association) number A_g gives the number of molecules (solvophobic monomer or tetramer) in one aggregate. Two solvophobic monomers are

supposed to belong to the same aggregate, if they are in contact, i.e., the distance between the centers of corresponding beads is lower than one reduced unit. Similarly, two solvophobic tetramers are supposed to belong to the same aggregate, if they have two or more contacts either with the solvophobic part of the dendrimer or with another already solubilized tetramer.

As the aggregates with different aggregation numbers are usually simultaneously present in the solution, the number distribution function of aggregation numbers or weight distribution function of aggregation numbers is used for the characterization of the system. The number distribution function $F_n(A_g)$ is defined as the number fraction of aggregates containing A_g molecules:

$$F_n(A_g) = \frac{N(A_g)}{\sum_i N_i(A_g)}, \tag{5.5}$$

where $N(A_g)$ is the number of aggregates consisting of A_g monomers, resp. tetramers, and $i = A_g$. The weight distribution function of aggregation numbers $F_w(A_g)$ is defined as:

$$F_w(A_g) = \frac{m_{A_g} N(A_g)}{\sum_i m_i N_i(A_g)}, \tag{5.6}$$

where m_{A_g} is the mass of an aggregate with aggregation number A_g and $i = A_g$.

The weight distribution function is also used for the description of solubilization capacity of dendrimer. Every solvophobic molecule, which forms an aggregate with dendrimer solvophobic core is considered as solubilized.

6 Results and discussion

General suitability of DPD method for studies of dendrimer behavior in solutions was proved within my bachelor thesis (2013) by correct reproduction of scaling law of the gyration radius of homopolymer dendrimer in good solvent. This work has also shown, that copolymer dendrimers are more suitable for solubilization of solvophobic compounds than homopolymers.

6.1 Solubilization of the solvophobic monomer

6.1.1 Solvophobic monomer without preferential interaction with dendrimer core

At first, the study of the interaction between dendrimer and solvophobic monomer at bead concentration $c = c_0$ was performed using the repulsion parameters listed in tab. 5.1. Only two values of repulsion parameters were used in this part of the thesis, as is obvious from the table.

The solubilization of the monomer in the dendrimer core was modeled as a process driven by solvophobic character of this monomer ($a_{(\mathrm{S|B})} > 25$). The interaction between beads of the monomer and dendrimer core was the same as the interaction between beads of the monomer.

The obtained results show, that when $a_{(\mathrm{S|B})} = 40$, only a few monomer beads are solubilized in the dendrimer core. The solubilization of solvophobic monomer in dendrimer core increases with increasing repulsion parameter a, but high values of repulsion parameter ($a = 50$) are experimentaly unrealistic. Furthermore, aggregation of monomer was observed at higher values of repulsion parameter and at the bead concentrations higher than c_0. It is because of huge solvophobicity of monomer, as shown the Fig. 6.1, where monomer precipitates from solution.

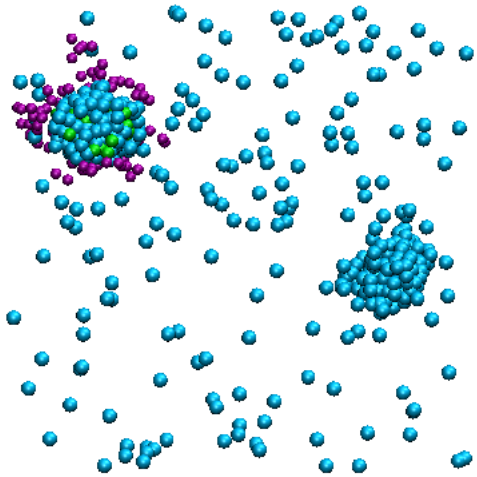

Figure 6.1: A snapshot of simulation box containing dendrimer $s = 7$, $g = 3$ and solvophobic monomer ($a_{(\mathrm{S|B})} = 50$; $c = 1.7c_0$).

The performed two-parameters-study has shown that the variation of two repulsion parameters does not allow to describe the real process of solubilization properly. The solvophobicity of the monomer alone is not sufficient condition for its preferential incorporation in dendrimer core. For this reason, the attractive interaction between solvophobic compound and the dendrimer core was applied in the model.

6.1.2 Solvophobic monomer with preferential interaction with dendrimer core

The non-realistic two-parameters-study was replaced by three-parameters-study, in which repulsive solvophobic interaction was kept constant (value $a = 40$) in all systems and the encapsulation of solvophobic monomer, resp. tetramer was promoted by the third parameter, which describes the attractive interaction between solvophobic monomer, resp. tetramer, and solvophobic dendrimer part – $a_{(\mathrm{B|A_1})} < 25$. The values of the used parameters are listed in table 5.2.

6.1.2.1 Effect of the box size

Because the simulations have been performed in a simulation box with periodic boundary conditions, it was necessary to prevent the possibility that the results of simulations could be affected by small box size and by periodicity. In the case of too small size of the simulation box, the dendrimer interacts due to periodic boundary

condition with its own image and the condition of infinite dilution is not fulfilled. For this reason, the simulations were performed in boxes with different L ($L = 20$, 22 and 30) and radial number bead densities were evaluated and mutually compared.

The comparison of radial number density of beads have proved that the results are the same for different box sizes as is shown in Fig. 6.2 and thus the size of the simulation box ($L = 22$ for $s = 5$) is large enough. Analogically, the size of the simulation box $L = 30$ is large enough for spacer $s = 7$.

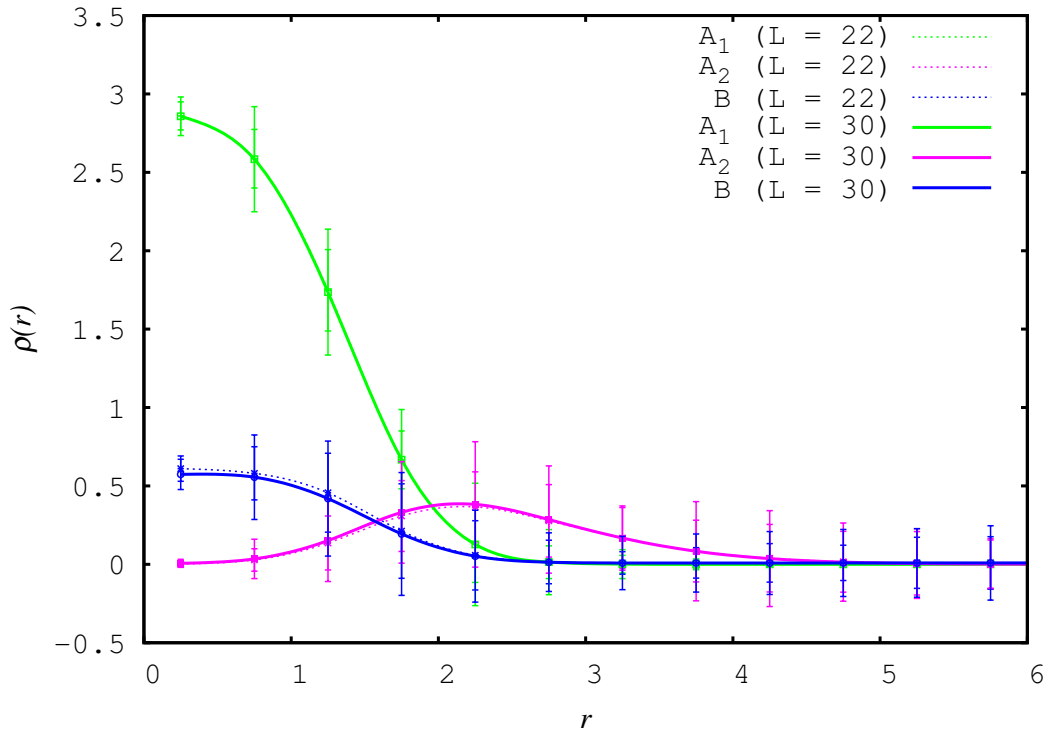

(a) $L = 20$ and $L = 22$

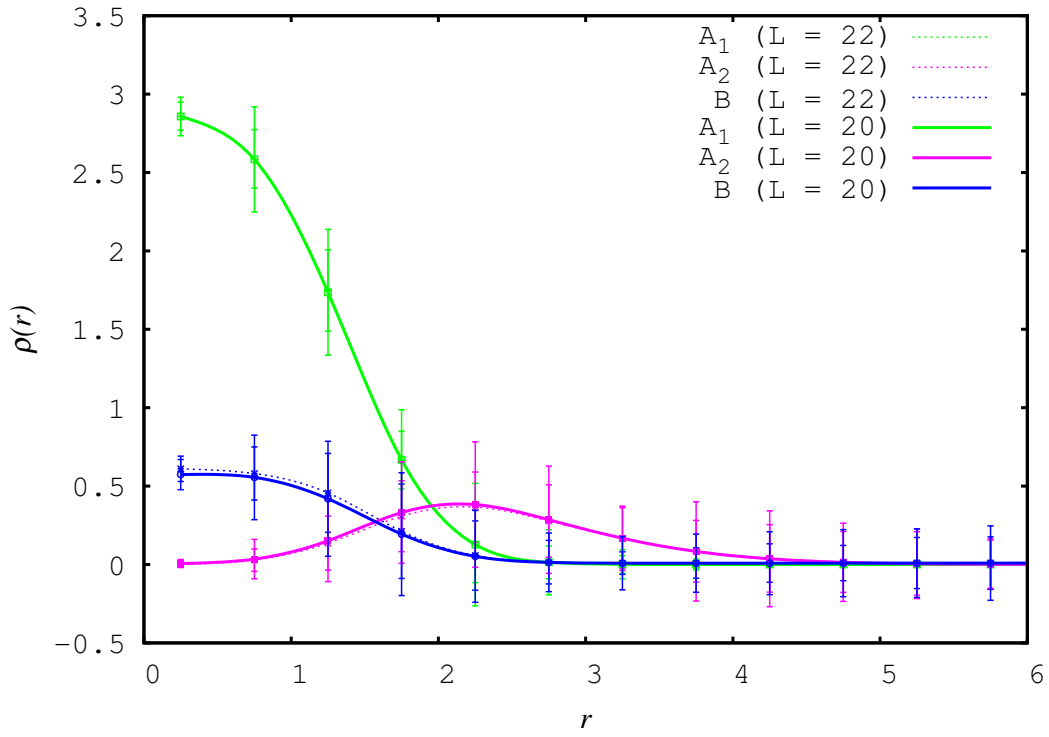

(b) $L = 22$ and $L = 30$

Figure 6.2: Segment densities of dendrimer solvophobic (A_1) and solvophilic (A_2) beads and beads of solvophobic monomer (B), $s = 5$, $g = 3$, $a_{(B|A_1)} = 20$, for several box sizes (a) $L = 20$ and $L = 22$, (b) $L = 22$ and $L = 30$. Green line is for A_1, purple for A_2 and blue one for B. Dashed lines are for $L = 22$, solid for $L = 20$ or 30.

6.1.2.2 Equilibration period

To find the appropriate length of the equilibration period, the simulations from three different initial conformation were performed and changes in the gyration radius of the inner solvophobic part $R_g(\mathrm{A}_1)$ were observed. For these simulations, the dendrimer with $s = 5$, $g = 3$, $a_{(\mathrm{B}|\mathrm{A}_1)} = 20$ was chosen and the bead concentration of solvophobic monomer was either $c = 0$ (copolymer were in pure solvent) or $c = c_0$.

For the dendrimer in pure solvent, the three initial conformations were chosen: random one, completely expanded and planar conformation with linear spacers, as is shown in Fig. 6.3. For the dendrimer in solution containing solvophobic monomer, the three initial conformations were chosen: random one, conformation containing huge amount of monomer solubilized in core and the expanded conformation without any solubilized monomer, as is shown in Fig. 6.4.

The dependence of the gyration radius of the dendrimer inner part $R_g(\mathrm{A}_1)$ on the number of simulation steps (see Figs. 6.3 and 6.4) was monitored. From Figs. 6.3 and 6.4 it is evident that the gyration radius quickly converges to the same constant value in all cases. According these results, the minimum equilibration period can be shorter than 5000 simulation steps. However, the equilibration period used in simulation runs was at least ten times longer to safety avoid the non-equilibrated states.

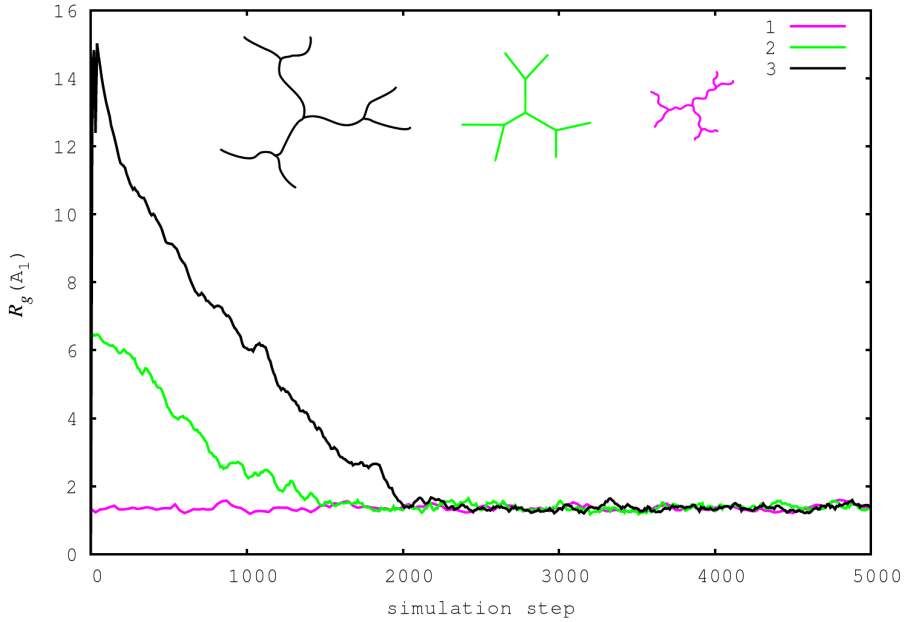

Figure 6.3: The evolution of the gyration radius of the inner part of dendrimer $R_g(\mathrm{A}_1)$, $s = 5$, $g = 3$ in pure solvent as a function of the simulation step from three different initial dendrimer conformations. Black curve is for the initial expanded conformation, green for planar one and purple for random one.

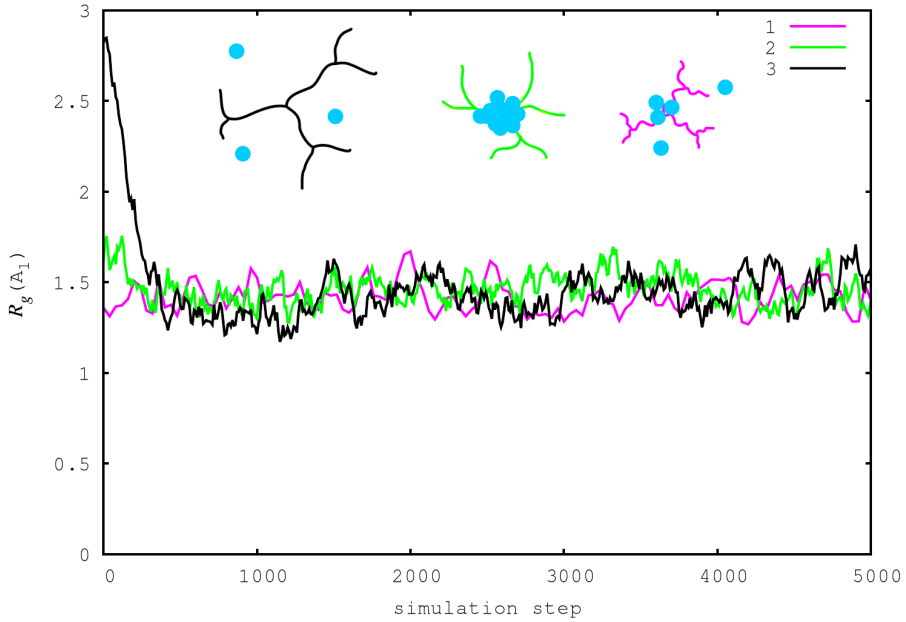

Figure 6.4: The evolution of the gyration radius of the inner part of dendrimer $R_g(\mathrm{A}_1)$, $s = 5$, $g = 3$, $a_{(\mathrm{B}|\mathrm{A}_1)} = 20$ in presence of solvophobic monomer, $c = c_0$, as a function of simulation step from three different initial dendrimer conformations. Black curve is for the initial expanded conformation without any solubilized monomer, green one is conformation containing huge amount of monomer and purple is random one.

6.1.2.3 Effect of the monomer concentration

The results of solubilization study based on the three-parameters-model and the most important trends concerning the size and inner structure of aggregates will be analysed and discussed with help of several different plots. In Fig. 6.6, the angularly averaged radial densities of dendrimers segments A_1, A_2 and of solvophobic monomer B are plotted as functions of the distance from the center of the mass, r, for two dendrimers with $s = 5$ and 7, for the constant concentration of the solvophobic monomer c_0 and different values of the repulsion parameter $a_{(B|A_1)}$.It is obvious that the results for $s = 5$ and 7 are qualitatively the same, only the densities of solvophobic monomer are little higher for the systems with spacer $s = 7$. Their solubilization capacity is higher, as expected from bigger size of the solvophobic core. From this reason, only the behavior of the dendrimers with spacer $s = 5$ will be discussed in the remaining part of this paragraph. Decreasing value of $a_{(B|A_1)}$, which emulates the increasing attraction between B and A_1 (as compared with the interaction between S and A_2) promotes the solubilization of B in the solvophobic core (A_1) of the dendrimer. The density of B indicates that the compound concentrates in the central part of the dendrimer (i.e., in the core) and the size of the core slightly increases. The density of A_2 segments does not almost change. Generally speaking, the changes of segment densities A_1 and A_2 are fairly small at this relatively low concentration of monomer.

In Fig. 6.7, the effect of increasing concentration of the solvophobic monomer on the inner structure of associates is depicted for two different interaction parameters $a_{(B|A_1)}$. To present a comprehensive picture of the behavior, the changes of concentration profiles of individual components B, A_1 and A_2 are shown in separate subsections of the figure. Figs. 6.7 (a) and (b) demonstrate efficient solubilization of the solvophobic monomer in dendrimer structures. The density of B segments in the central part is fairly high (as expected, it is higher for $a_{(B|A_1)} = 20$ than for $a_{(B|A_1)} = 22.5$). Because A_1 segments are partially replaced by segments B, their density decreases in the central part and some segments are pushed farther from the dendrimer center. The solubilization thus causes the expansion of the core (see the broadening of density profiles with increasing c in Figs. 6.7 (c) and (d)). The distance of stabilizing segments A_2 from the center of the mass also increases

with increasing c as it is witnessed by changes in their density profiles (by shifts of their maxima in density profiles towards larger r). The comparison of B and A_1 density profiles is very interesting. It reveals that for higher concentrations, a non-negligible fraction of solvophobic monomer condense on the A_1 core surface (i.e., in the A_2 shell). The non-negligible overlap of B and A_2 density profiles suggests the intermixing of corresponding blocks, but it is mostly the artifact of the angular averaging. The snapshots (see Figs. 6.5) show that the solvophobic beads stick and literally »glue« to a relatively compact »cloud« of B molecules already condensed in the central region. The stabilizing A_2 branches are preferentially radially stretched. They pass the region filled with the »glued« solvophobic monomers, but the actual intermixing of B and A_2 is limited.

The observation of weight function of aggregation numbers shows (see Fig. 6.8), that only a few solvophobic monomers create aggregates even for higher bead concentrations. These small aggregates remain in solution independently on presence of dendrimer (Fig. 6.5).

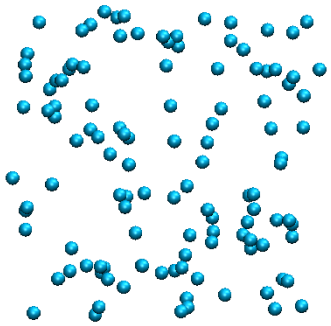

(a) $c = c_0$

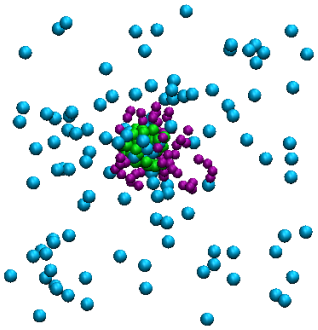

(b) $c = c_0$

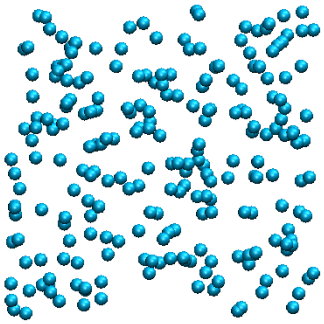

(c) $c = 2.0c_0$

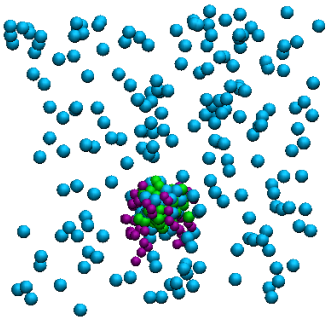

(d) $c = 2.0c_0$

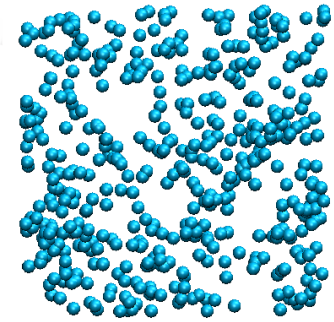

(e) $c = 4.0c_0$

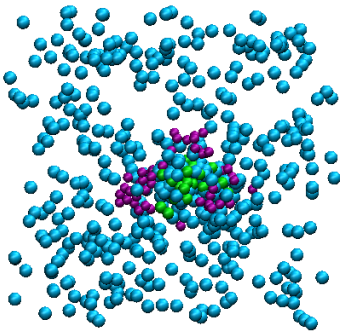

(f) $c = 4.0c_0$

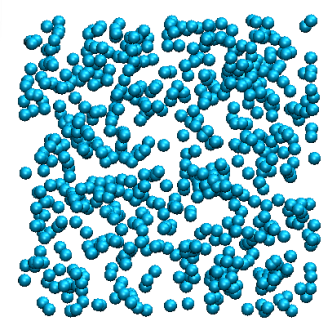

(g) $c = 6.0c_0$

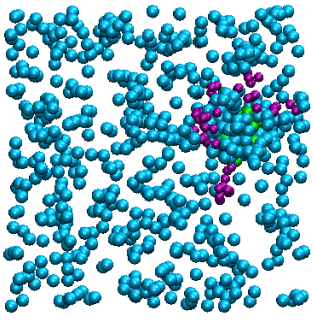

(h) $c = 6.0c_0$

Figure 6.5: Snapshots of solvophobic monomer with different concentration c. The left column is for the solvophobic monomer without dendrimer and the right column depicted solubilization of monomer in the dendrimer $s = 5$, $g = 3$ and $a_{(\mathrm{B}|\mathrm{A}_1)} = 20$.

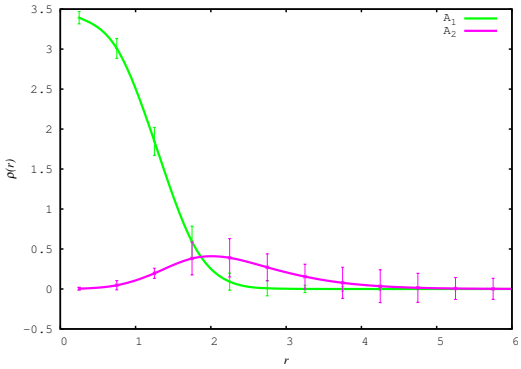

(a) $s = 5$, pure solvent

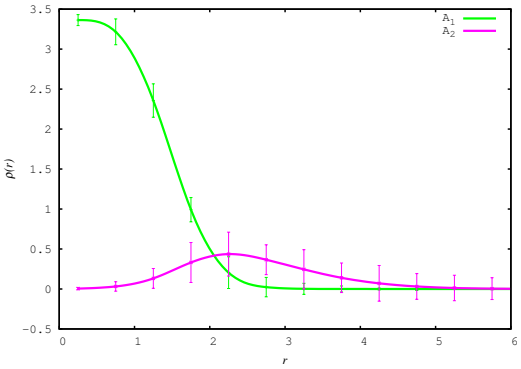

(b) $s = 7$, pure solvent

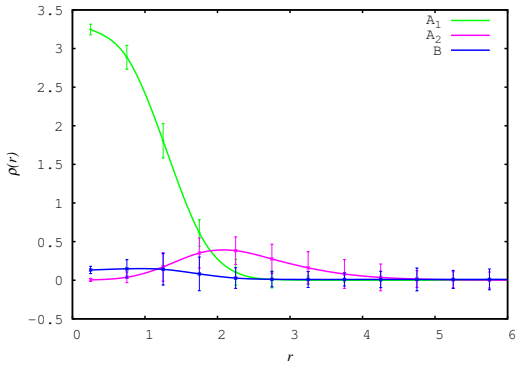

(c) $s = 5$, $a_{(\mathrm{B}|\mathrm{A}_1)}$=25

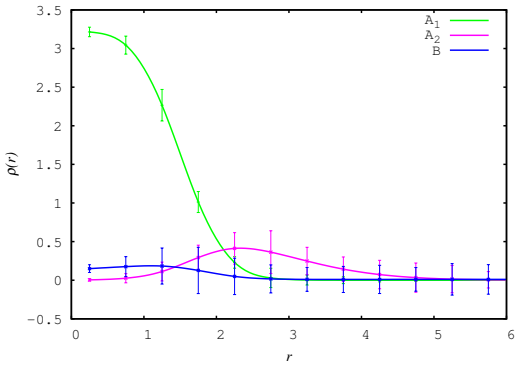

(d) $s = 7$, $a_{(\mathrm{B}|\mathrm{A}_1)}$=25

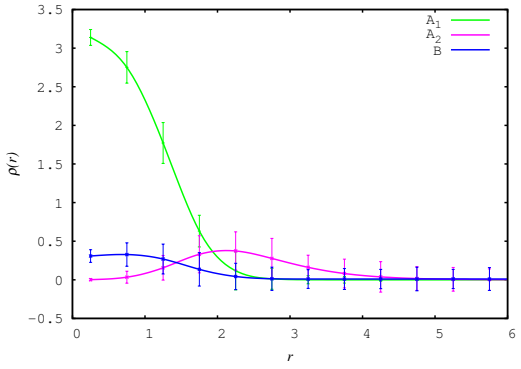

(e) $s = 5$, $a_{(\mathrm{B}|\mathrm{A}_1)}$=22.5

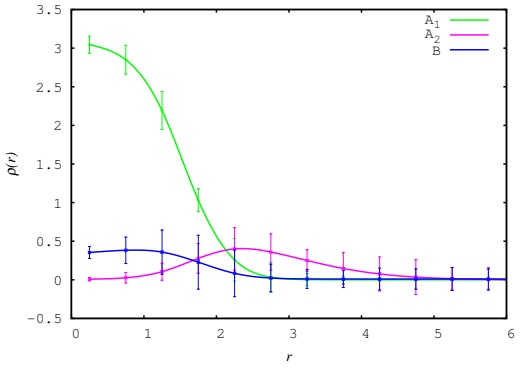

(f) $s = 7$, $a_{(\mathrm{B}|\mathrm{A}_1)}$=22.5

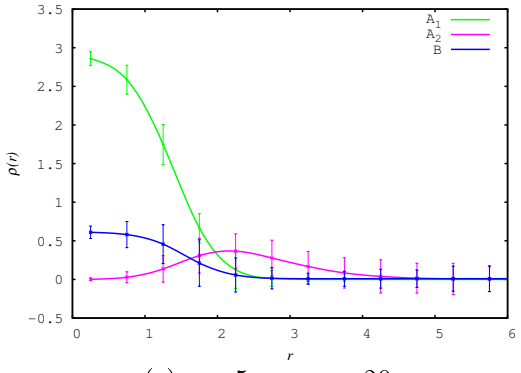

(g) $s = 5$, $a_{(\mathrm{B}|\mathrm{A}_1)}$=20

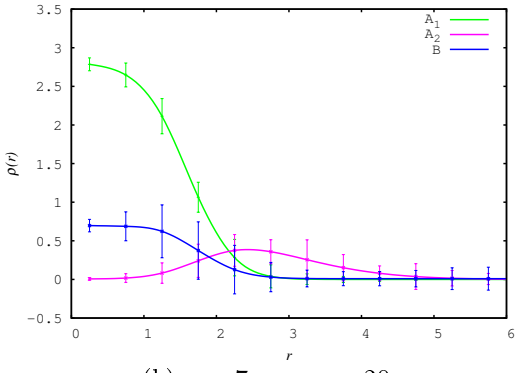

(h) $s = 7$, $a_{(\mathrm{B}|\mathrm{A}_1)}$=20

Figure 6.6: The copolymer bead densities of dendrimer with $s = 5$ and 7, $g = 3$ and different values of $a_{(\mathrm{B}|\mathrm{A}_1)} = 20$, 22.5 and 25 for system: (a), (b) without any solvophobic monomer, (c) – (h) containing solvophobic monomer with total bead concentration $c = c_0$. The green line corresponds to A_1, purple to A_2 and blue to B.

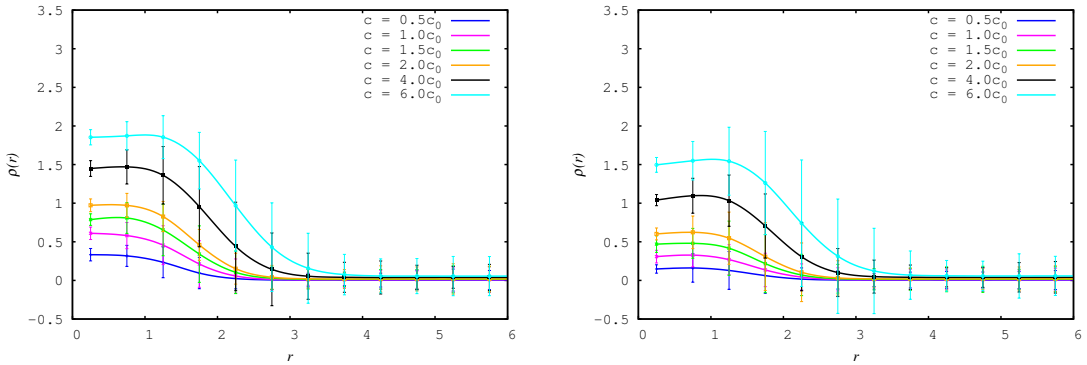

(a) B; $a_{(\mathrm{B}|\mathrm{A}_1)} = 20$

(b) B; $a_{(\mathrm{B}|\mathrm{A}_1)} = 22.5$

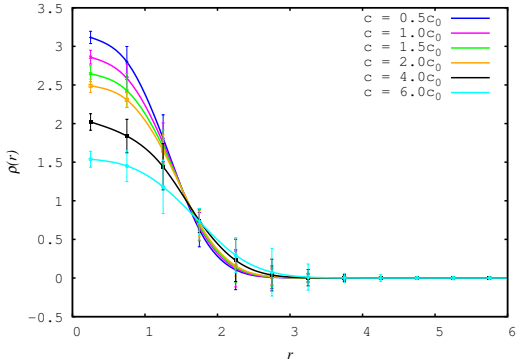

(c) A_1; $a_{(\mathrm{B}|\mathrm{A}_1)} = 20$

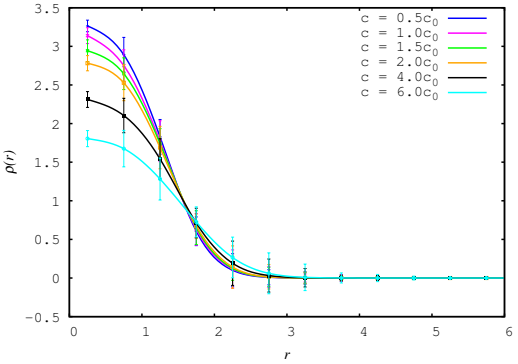

(d) A_1; $a_{(\mathrm{B}|\mathrm{A}_1)} = 22.5$

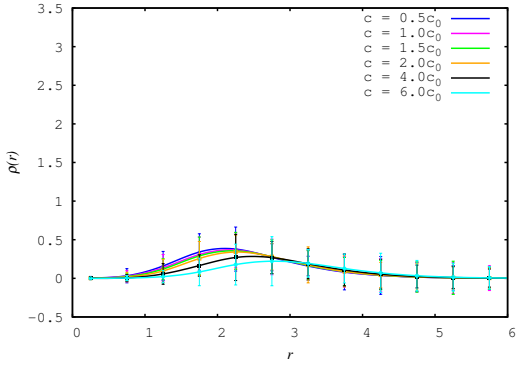

(e) A_2; $a_{(\mathrm{B}|\mathrm{A}_1)} = 20$

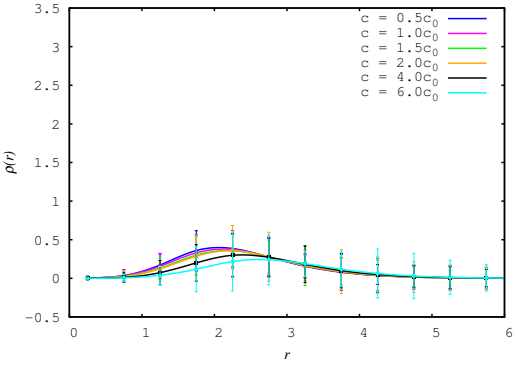

(f) A_2; $a_{(\mathrm{B}|\mathrm{A}_1)} = 22.5$

Figure 6.7: The bead densities for solvophobic monomer (first row), solvophobic part of dendrimer (second row) and solvophilic part of dendrimer (third row) $s = 5$, $g = 3$ for increasing total bead concentration c. The blue lines correspond to the concentration $c = 0.5c_0$, purple lines to $c = c_0$, green lines to $c = 1.5c_0$, orange line to $c = 2.0c_0$, black lines to $c = 4.0c_0$ and cyan lines to $c = 6.0c_0$. The left column is for $a_{(\mathrm{B}|\mathrm{A}_1)} = 20$, the right for $a_{(\mathrm{B}|\mathrm{A}_1)} = 22.5$.

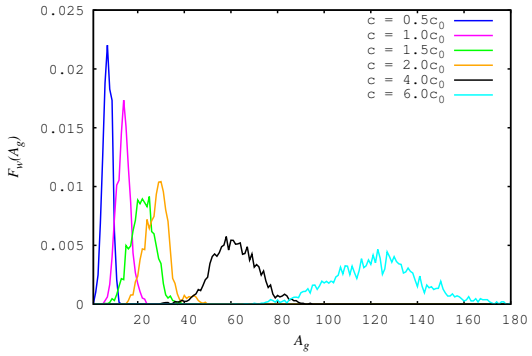

(a) Monomer solubilized in the dendrimer; $a_{(\mathrm{B|A_1})} = 20$

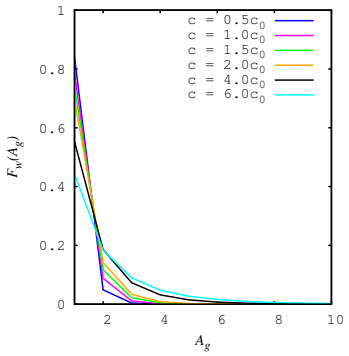

(b) Non-solubilized monomer

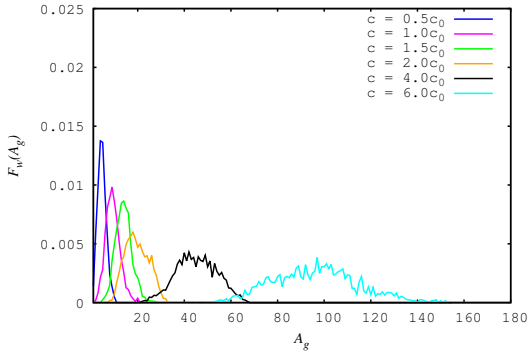

(c) Monomer solubilized in the dendrimer; $a_{(\mathrm{B|A_1})} = 22.5$

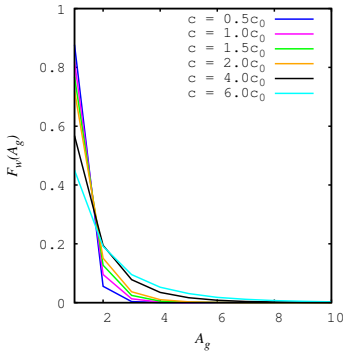

(d) Non-solubilized monomer

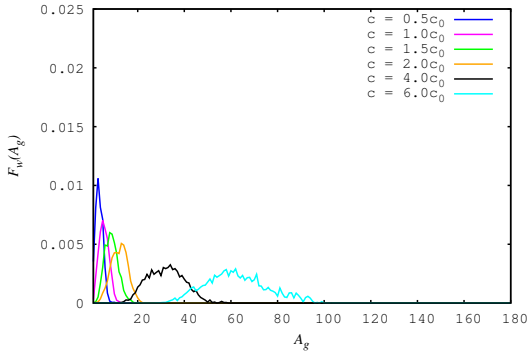

(e) Monomer solubilized in the dendrimer; $a_{(\mathrm{B|A_1})} = 25$

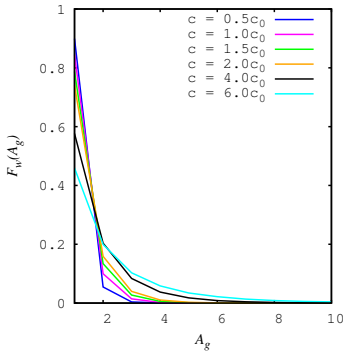

(f) Non-solubilized monomer

Figure 6.8: The weight distribution function $F_w(A_g)$ of aggregation number A_g for dendrimer $s = 5$, $g = 3$, $a_{(\mathrm{B|A_1})} = 20$ (the first raw), 22.5 (the second raw) and 25 (the third raw) for systems containing dendrimer and solvophobic monomers with different bead concentrations. The left column is for solvophobic monomer solubilized in the dendrimer, the right column for the aggregates of non-solubilized solvophobic beads. The colors of the individual curves are the same as in Fig. 6.7.

6.1.2.4 Protection effect of the solvophilic dendrimer part

The dendrimers with two solvophobic (A_1 type beads) and two solvophilic (A_2 type beads) generations and with the same spacer length for all generations $s = 5$ were simulated for $a_{(B|A_1)} = 20$ and for different bead concentration of monomer c.

The bead densities for the four-generations-dendrimer and the three-generations-dendrimer in pure solvent ($c = 0$) are shown in Fig. 6.9. The behavior of this four-generations-dendrimer in pure solvent is similar to the three-genera/tions-dendrimer as is demonstrated by number bead densities of dendrimer segments (see Fig. 6.9). The addition of the fourth solvophilic generation leads to broadening of A_2 bead density with slightly higher maximum, because the number of solvophilic segments of four-generations-dendrimer is three time higher than the number of solvophilic segments of the three-generations-dendrimer. The number of the solvophobic segments is the same for both dendrimer types and the corresponding bead densities differ only in the centre in accordance with published data. [37]

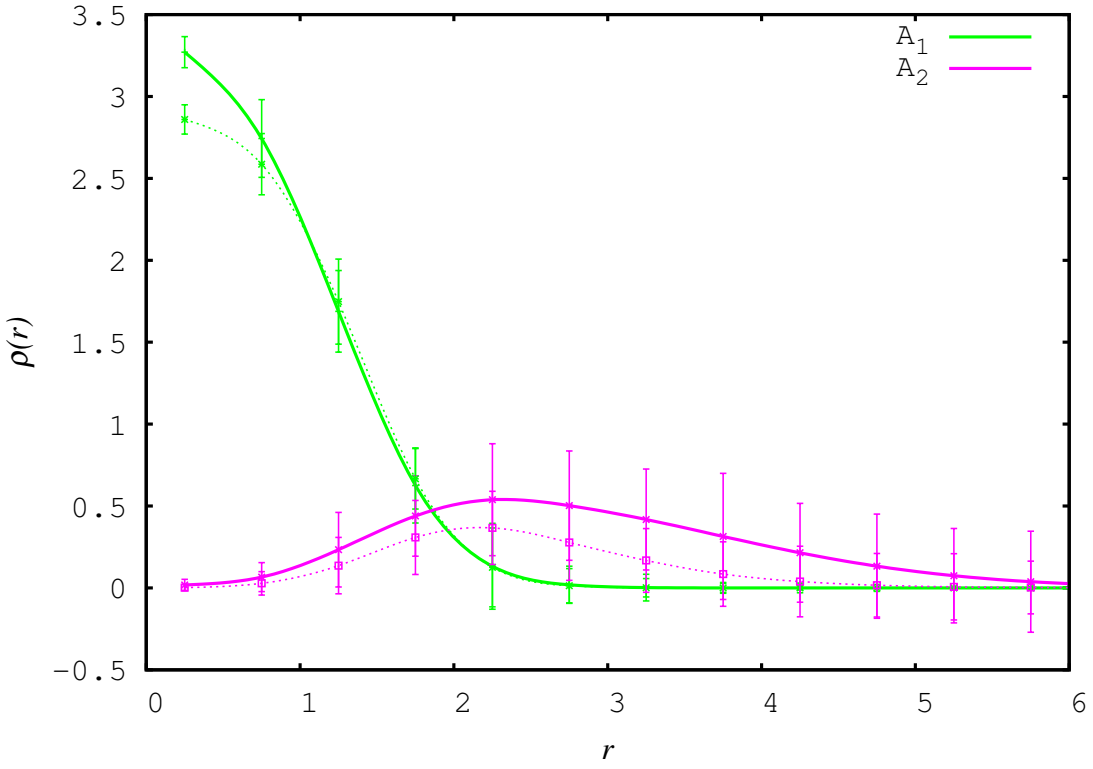

Figure 6.9: Bead densities for dendrimer in pure solvent ($c = 0$) as function of distance from the center of mass. Solid lines are for dendrimer with $s = 5$, $g = 4$, dashed for $s = 5$, $g = 3$. Purple line is for densities of A_1 beads, green line is for A_2 beads.

Bead densities of dendrimer segments and solvophobic monomer as a function of the distance from the center of mass are depicted for two monomer concentrations ($c = c_0$ and $c = 2.0c_0$) in Fig. 6.10 for the both dendrimer types. The solvophobic bead densities of the four-generations-dendrimer and the three-generations-dendrimer are for both concentrations similar, however the corresponding densities of solvophobic monomer differ significantly. The increase of the number of solvophilic segments A_2 in the four-generations-dendrimer improves the protection of dendrimer core surface against the solvent molecules. As the interaction of the solvophobic monomers with solvent is the same as with the solvophilic dendrimer segments and the covering of the dendrimer core is better, the solvophobic monomer density is lower on the surface of the dendrimer core and also inside in the core. The change of the solvophilic segment densities against the pure solvent is for these concentrations negligible.

The weight distribution functions of aggregation numbers for both dendrimer types and two monomer concentrations are shown in Fig. 6.11. The addition of one more solvophobic generation suppressed the solubilization of monomer segments in the dendrimer; the maximum value of weight distribution function is lower and is shifted to lower aggregation number. Time evolution of the solubilization of monomer in the dendrimer is illustrated also by Fig. 6.12.

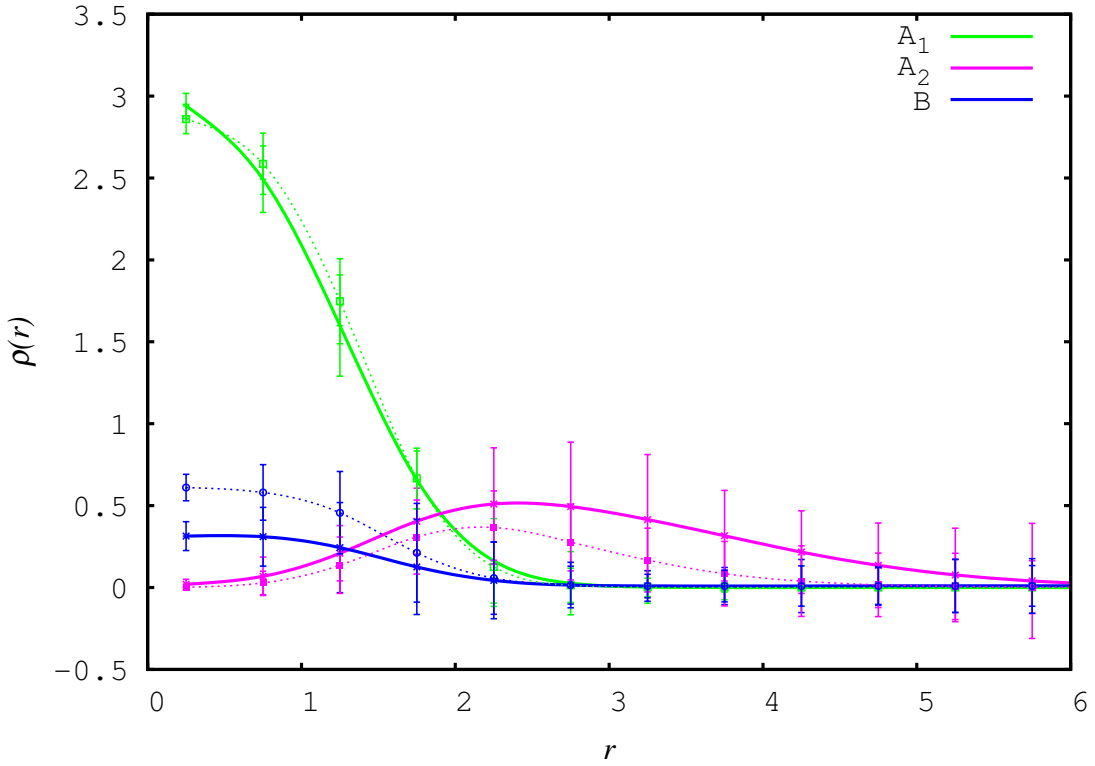

(a) $c = c_0$

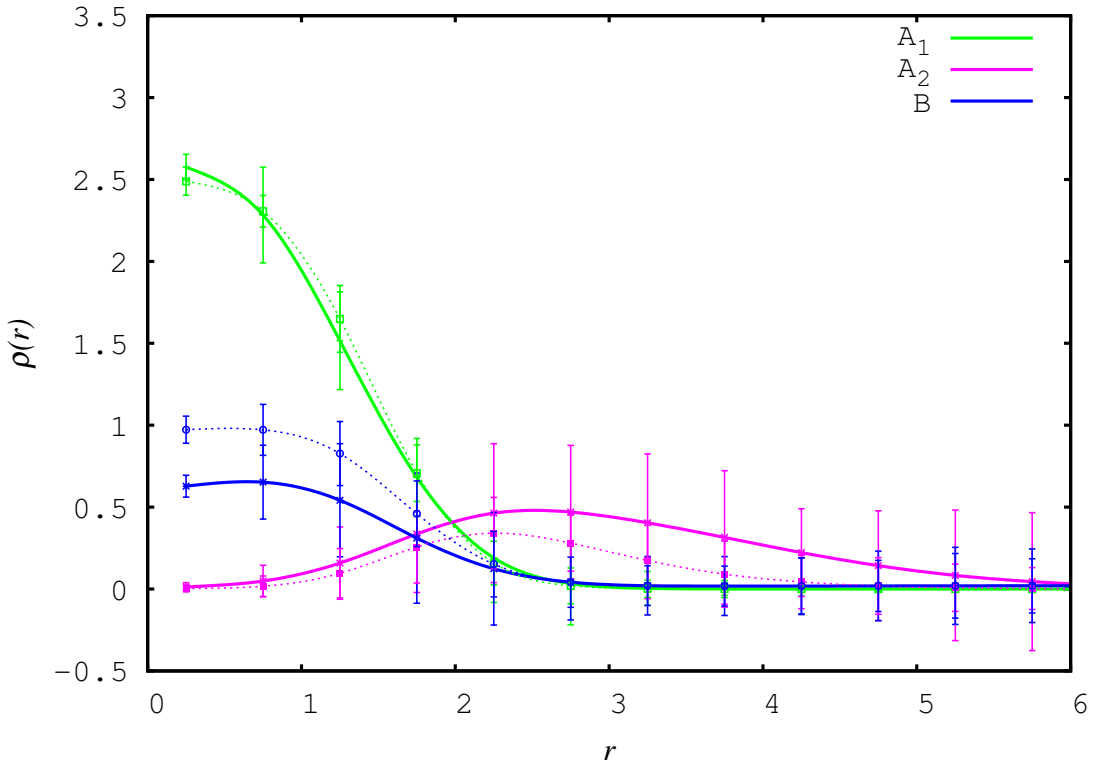

(b) $c = 2.0c_0$

Figure 6.10: The bead densities of dendrimer with $s = 5$, $g = 4$ and $a_{(\mathrm{B}|\mathrm{A}_1)} = 20$ as a function of distance from the center of mass for different total bead concentrations of monomer c: (a) $c = c_0$, (b) $c = 2.0c_0$, depicted by solid lines. Dashed lines corresponds to the systems of the three-generations-dendrimer under the same conditions.

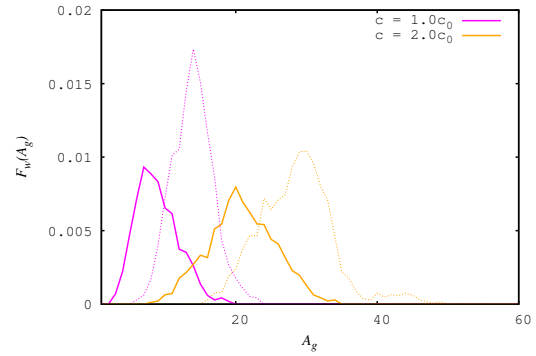

(a) Monomer solubilized in the dendrimer; $a_{(\mathrm{B|A_1})} = 20$

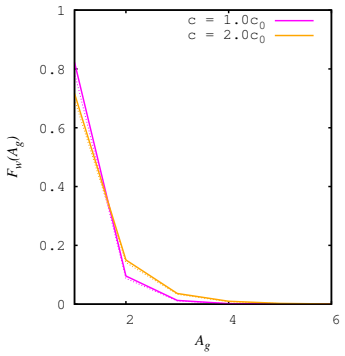

(b) Non-solubilized monomer

Figure 6.11: The weight distribution function $F_w(A_g)$ of aggregation number A_g for dendrimers $s = 5$, $g = 4$, $a_{(\mathrm{B|A_1})} = 20$ for monomer concentration $c = c_0$ (solid purple line) and $c = 2.0c_0$ (solid orange line). The left column is for solvophobic monomer solubilized in the dendrimer, the right column for the aggregates of non-solubilized solvophobic beads. Dashed lines are for the three-generations-dendrimer under the same conditions.

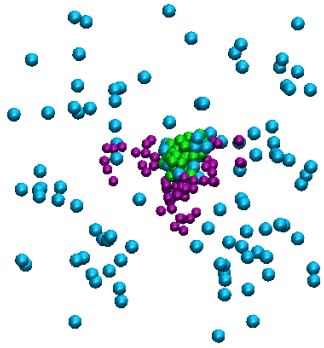

(a) Simulation step = $1.0 \cdot 10^4$

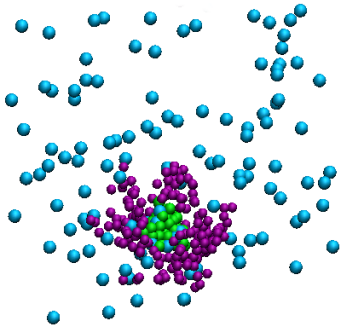

(b) Simulation step = $1.0 \cdot 10^4$

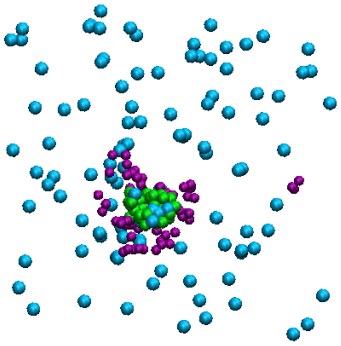

(c) Simulation step = $5.0 \cdot 10^4$

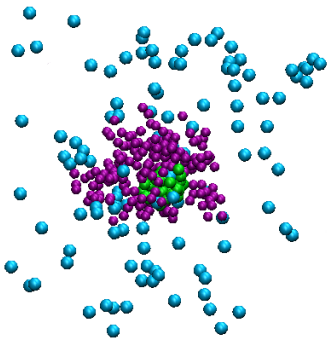

(d) Simulation step = $5.0 \cdot 10^4$

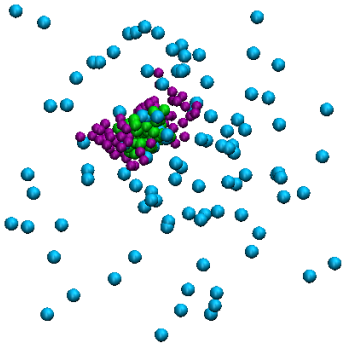

(e) Simulation step = $1.0 \cdot 10^5$

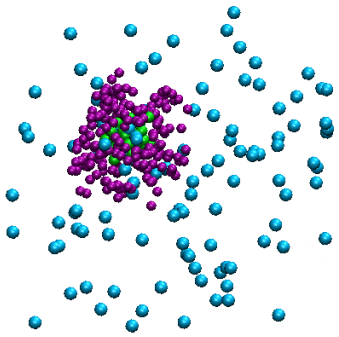

(f) Simulation step = $1.0 \cdot 10^5$

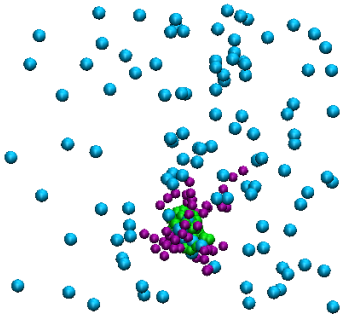

(g) Simulation step = $1.5 \cdot 10^5$

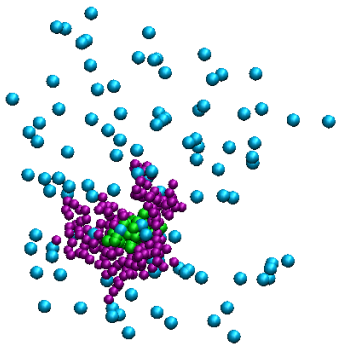

(h) Simulation step = $1.5 \cdot 10^5$

Figure 6.12: Time evolutions of the simulation box. The left column depicted solubilization of the solvophobic monomer ($c = c_0$) in the three-generations-dendrimer ($s = 5$, $a_{(\mathrm{B}|\mathrm{A}_1)} = 20$), the right depicted solubilization in the four-generations dendrimer ($s = 5$, $a_{(\mathrm{B}|\mathrm{A}_1)} = 20$).

6.2 Solubilization of the solvophobic tetramer

Solvophobic tetramer were modeled as four solvophobic beads connected in linear chain, as well as dendrimer, by harmonic spring potential with $r_0 = 0$, $k_S = 4$.

6.2.1 Solvophobic tetramer with preferential interaction with dendrimer core

6.2.1.1 Effect of the tetramer concentration

For the selected system (dendrimer with spacer $s = 5$, $g = 3$ and $a_{(\mathrm{B}|\mathrm{A}_1)} = 20$), the simulations of the solvophobic tetramer solubilization were performed to study the effect of the size of solubilized compound. The number of beads in simulation box corresponding to the reference total bead concentration c_0 for these systems was 120, as this number is divisible by four. The difference between this total bead concentration and the total bead concentration for monomer (118 beads in simulation box) is less than 2 %, so it is negligible.

In Fig. 6.13, the radial number densities of A_1 and A_2 segment of dendrimer and beads of solvophobic tetramer and monomer are depicted for different total bead concentration. It is obvious, that density of tetramer beads near the center of mass is appreciably higher than that of monomer. As in the case of the solubilization of the monomer, A_1 type beads are partially replaced by B types, their densities decreases near the center of mass and some segments are pushed farther, thus dendrimer core is expanding. The expanding core also influences A_2 beads density profiles. They have lower maxima shifted toward larger distance.

Similarly as monomer at higher concentrations, the tetramer beads also condense on the dendrimer core surface (see Fig. 6.13). However, the condensation of solvophobic tetramers occurs at lower total bead concentration than the condensation of monomers. This effect can be explained by four times higher attraction of tetramer to the dendrimer core. The connection of beads into tetramer increases also the mutual attraction of solvophobic tetramers and their solution behavior significantly differs from monomer behavior. In solutions without dendrimer, the tetramers precipitate even at very low concentration. However, the tetramer precipitates are solubilized in the dendrimer if the dendrimer is present in the solution (Figs. 6.14 and 6.15).

This picture is supported also by weight distribution functions of aggregation numbers (Fig. 6.16), which show that only a few non-aggregate tetramers stay in solution.

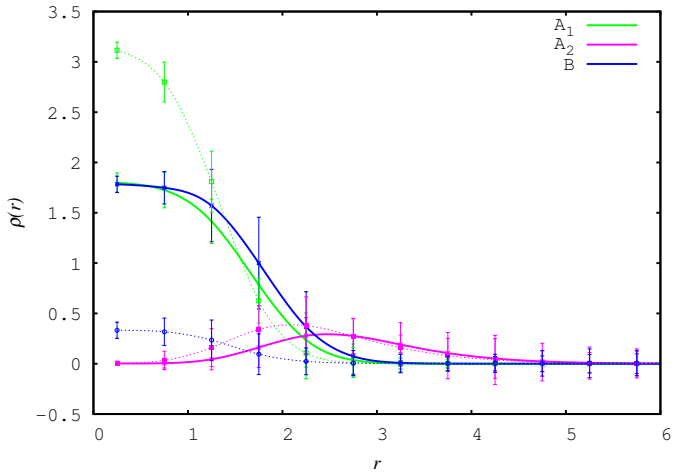

(a) $c = 0.5c_0$

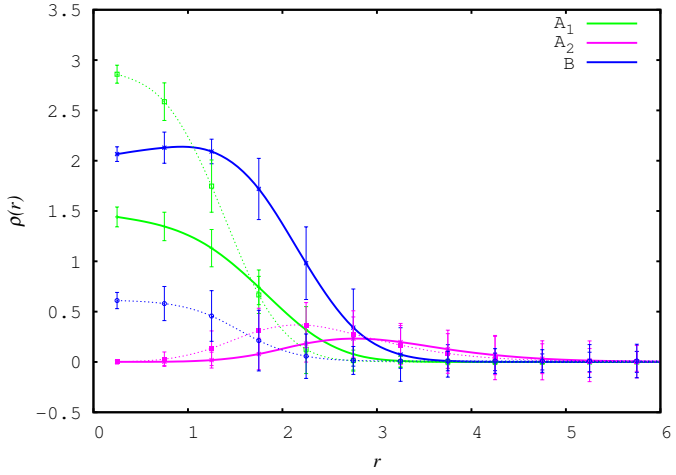

(b) $c = c_0$

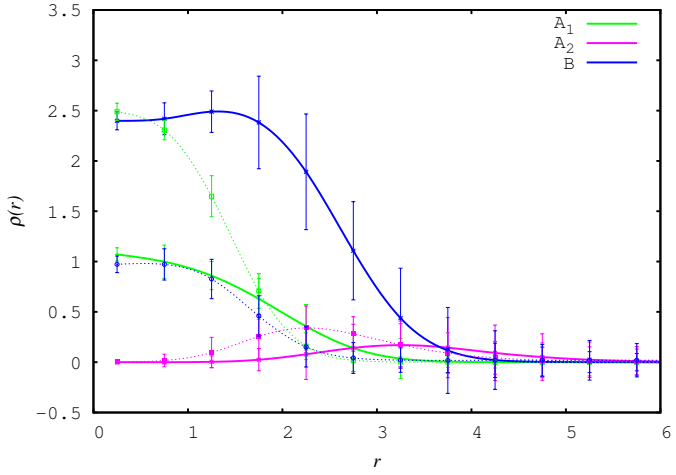

(c) $c = 2.0c_0$

Figure 6.13: The densities of beads of dendrimer with $s = 5$, $g = 3$ and $a_{(\mathrm{B}|\mathrm{A}_1)} = 20$ and solvophobic tetramer for different total bead concentration of tetramer c: (a) $c = 0.5c_0$, (b) $c = c_0$, (c) $c = 2.0c_0$, depicted by solid lines. Dashed lines corresponds to the systems containing solvophobic monomer under the same conditions.

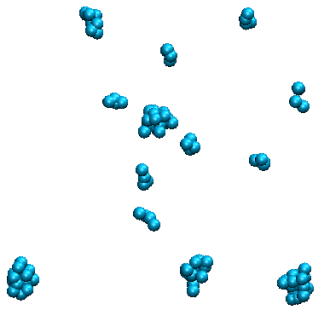

(a) Simulation step = $1.0 \cdot 10^4$

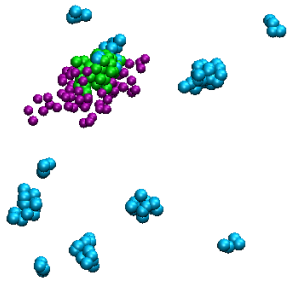

(b) Simulation step = $1.0 \cdot 10^4$

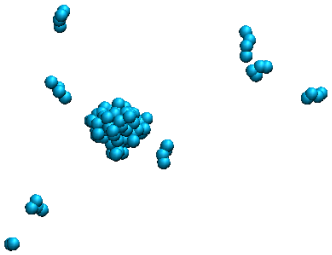

(c) Simulation step = $5.0 \cdot 10^4$

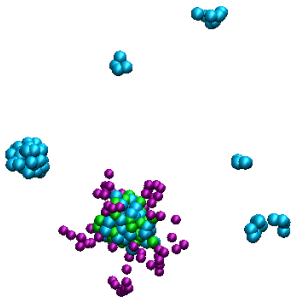

(d) Simulation step = $5.0 \cdot 10^4$

(e) Simulation step = $1.0 \cdot 10^5$

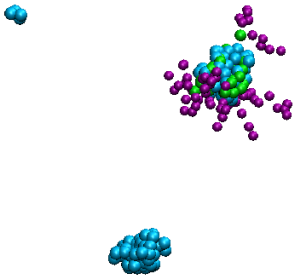

(f) Simulation step = $1.0 \cdot 10^5$

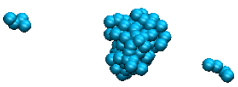

(g) Simulation step = $1.5 \cdot 10^5$

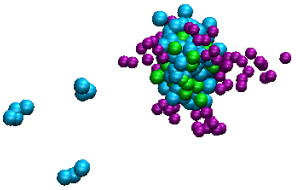

(h) Simulation step = $1.5 \cdot 10^5$

Figure 6.14: Time evolution of simulation box. The left column depicted the solvophobic tetramer ($c = c_0$). The right column depicted the solvophobic tetramer ($c = c_0$) and dendrimer ($s = 5$, $g = 3$, $a_{(\mathrm{B}|\mathrm{A}_1)} = 20$).

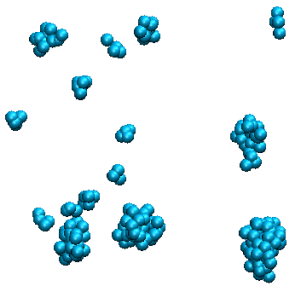

(a) Simulation step = $1.0 \cdot 10^4$

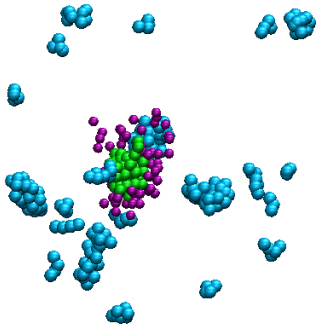

(b) Simulation step = $1.0 \cdot 10^4$

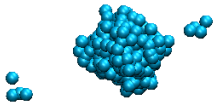

(c) Simulation step = $5.0 \cdot 10^4$

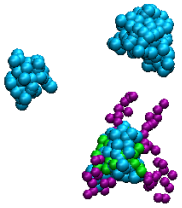

(d) Simulation step = $5.0 \cdot 10^4$

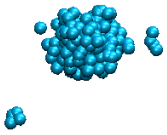

(e) Simulation step = $1.0 \cdot 10^5$

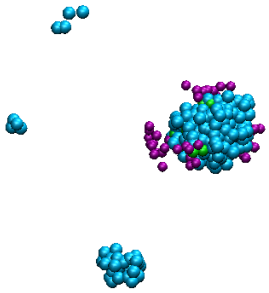

(f) Simulation step = $1.0 \cdot 10^5$

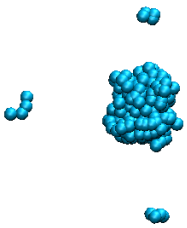

(g) Simulation step = $1.5 \cdot 10^5$

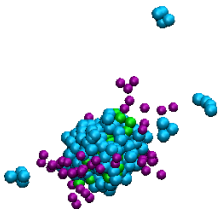

(h) Simulation step = $1.5 \cdot 10^5$

Figure 6.15: Time evolution of simulation box. The left column depicted the solvophobic tetramer ($c = 2.0c_0$). The right column depicted the solvophobic tetramer ($c = 2.0c_0$) and dendrimer ($s = 5$, $g = 3$, $a_{(\mathrm{B}|\mathrm{A}_1)} = 20$).

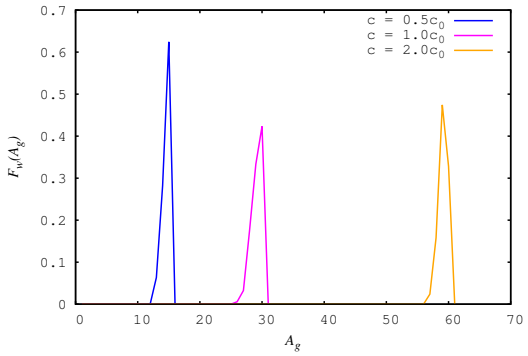

(a) tetramer solubilized in the dendrimer; $a_{(\mathrm{B}|\mathrm{A}_1)} = 20$

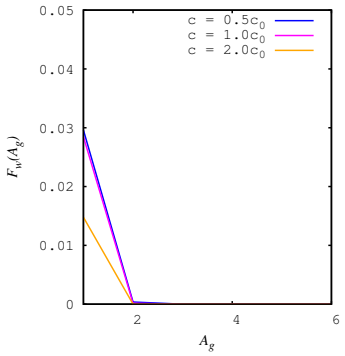

(b) Non-solubilized tetramer

Figure 6.16: The weight distribution function $F_w(A_g)$ of aggregation number A_g for dendrimers $s = 5$, $g = 3$, $a_{(\mathrm{B}|\mathrm{A}_1)} = 20$ for systems containing different concentration c of the solvophobic tetramer. The left column is for solvophobic tetramer solubilized in the dendrimer, the right column for the aggregates of non-solubilized solvophobic beads. The colors of the individual curves are the same as in Fig. 6.7.

6.2.1.2 Protection effect of the solvophilic dendrimer part

Radial number densities for the four-generations-dendrimer and the three-generations-dendrimer and two different total bead concentrations are depicted in Fig. 6.17. The number densities and also weight function of aggregation numbers (see Fig. 6.18) show significantly different behavior of tetramer and monomer for all concentrations. The radial density of solvophobic tetramer in the core of the four-generations-dendrimer is smaller than in the three-generations-dendrimer, but the difference is much more smaller than for monomer. Based on the time evolution of simulations box (Figs. 6.19 and 6.20) and the weigh distribution function of aggregation numbers (Fig. 6.18), it is obvious, that differences in densities between tetramer solubilized in the four-generations-dendrimer and three-generations-dendrimer is caused only by angularly averaging of densities and by their averaging over the all aggregation numbers rather than by protective effect of the additional solvophilic generation. The copolymer dendrimer with more than two solvophilic generations and/or with longer spacers has to be used to obtain the similar behavior as for monomer solubilization.

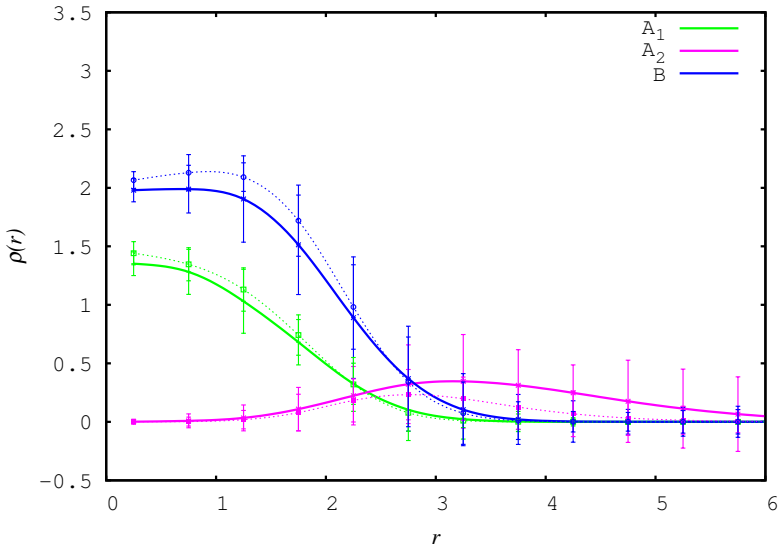

(a) $c = c_0$

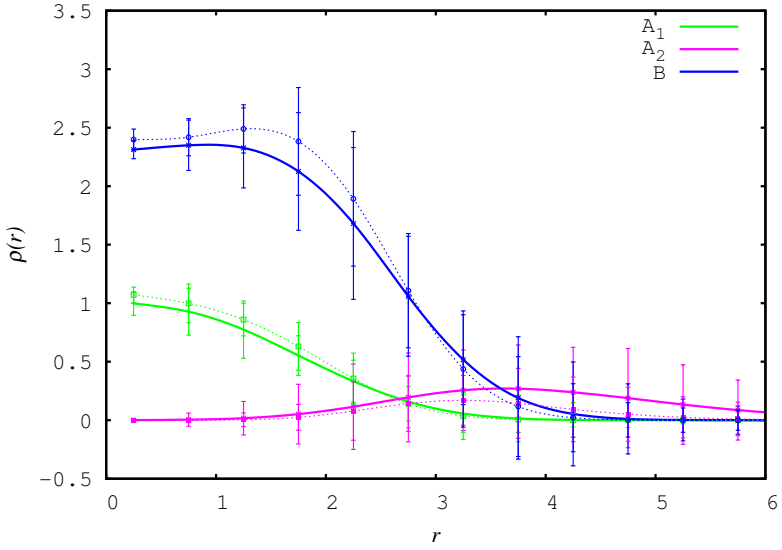

(b) $c = 2.0c_0$

Figure 6.17: Bead densities of dendrimer with $s = 5$, $g = 4$ and $a_{(\mathrm{B}|\mathrm{A}_1)} = 20$ and solvophobic tetramer for different total bead concentration$c$: (a) $c = c_0$, (b) $c = 2.0c_0$, depicted by solid lines. Dashed lines corresponds to the systems of the three generation dendrimer under the same conditions.

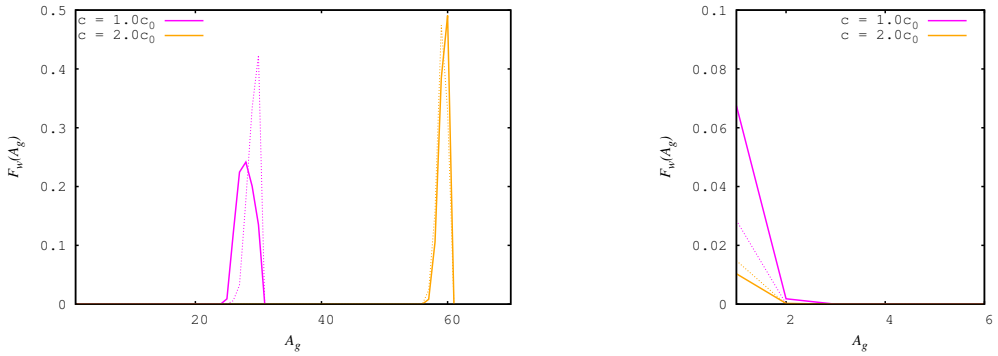

(a) Tetramer solubilized in the dendrimer; $a_{(\mathrm{B}|\mathrm{A}_1)} = 20$

(b) Non-solubilized tetramer

Figure 6.18: The weight distribution function $F_w(A_g)$ of aggregation number A_g for dendrimers $s = 5$, $g = 4$, $a_{(\mathrm{B}|\mathrm{A}_1)} = 20$ for different total bead concentration $c = c_0$ (purple line) and $c = 2.0c_0$ (orange) solvophobic tetramer. The left column is for solvophobic tetramer solubilized in the dendrimer, the right column for the aggregates of non-solubilized solvophobic beads. Dashed lines are for the three dendrimer under the same conditions.

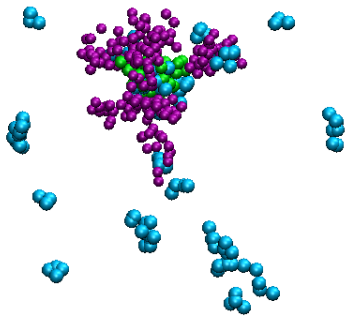

(a) Sim. step = $1.0 \cdot 10^4$

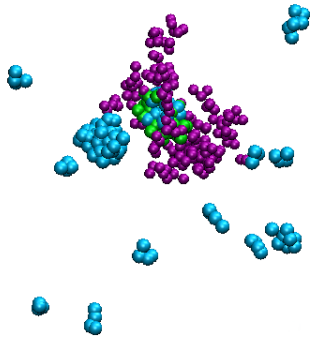

(b) Sim. step = $2.5 \cdot 10^4$

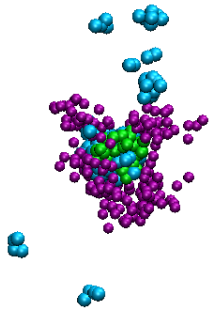

(c) Sim. step = $5.0 \cdot 10^4$

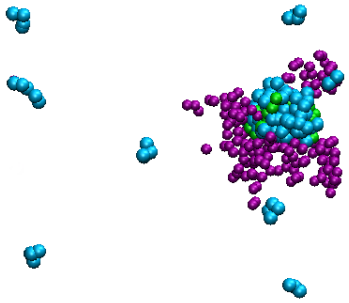

(d) Sim. step = $7.5 \cdot 10^4$

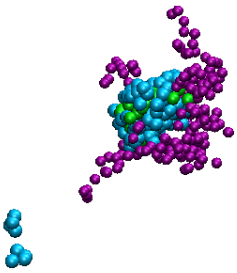

(e) Sim. step = $1.0 \cdot 10^5$

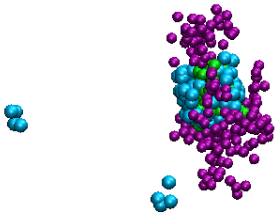

(f) Sim. step = $1.25 \cdot 10^5$

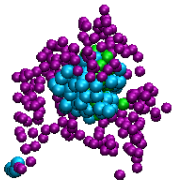

(g) Sim. step = $1.5 \cdot 10^5$

Figure 6.19: Time evolution of copolymer ($s = 5$, $g = 4$, $a_{(\mathrm{B}|\mathrm{A}_1)} = 20$) and solvophobic tetramer ($c = c_0$).

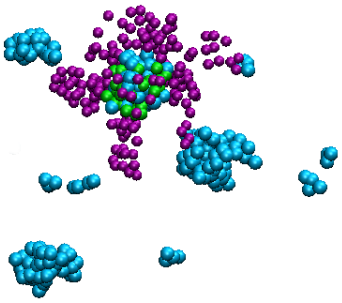

(a) Sim. step = $1.0 \cdot 10^4$

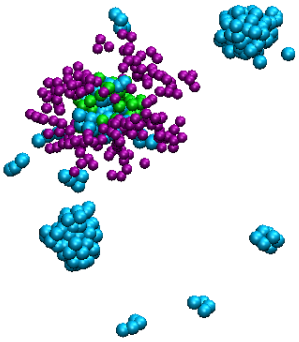

(b) Sim. step = $2.5 \cdot 10^4$

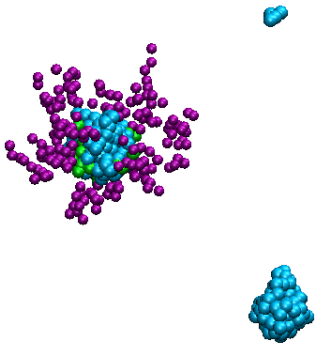

(c) Sim. step = $5.0 \cdot 10^4$

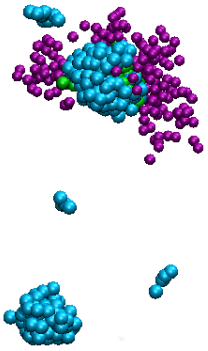

(d) Sim. step = $7.5 \cdot 10^4$

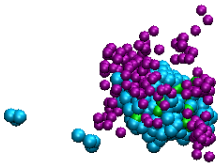

(e) Sim. step = $1.0 \cdot 10^5$

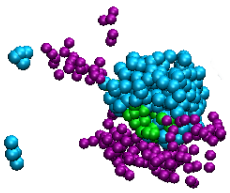

(f) Sim. step = $1.25 \cdot 10^5$

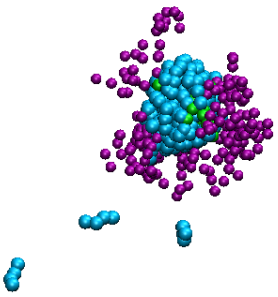

(g) Sim. step = $1.5 \cdot 10^5$

Figure 6.20: Time evolution of copolymer ($s = 5$, $g = 4$, $a_{(\mathrm{B}|\mathrm{A}_1)} = 20$) and solvophobic tetramer ($c = 2.0c_0$).

7 Conclusions

The behavior of the block copolymer dendrimers in solutions containing solvophobic compound was studied via dissipative particle dynamics. The dendrimer has the inner solvophobic part (two generations) protected by outer solvophilic part (one, resp. two generations). The interaction of solvophobic copolymer part with solvent was the same as the interaction of solvophobic compound with the solvent. Two types of solvophobic compound were studied – monomer and tetramer formed from four monomer beads under the same conditions.

The solubilization of solvophobic compounds in the copolymer dendrimer depends on the interaction between solvophobic part of dendrimer and solvophobic compound. When the solubilization is only due to the solvophobicity of the solvophobic compound (monomer), the precipitation of solvophobic compound from the solution occurs before its solubilization. To obtain demanded solubilization, preferential attractive interaction between the solvophobic part of dendrimer and solvophobic compound has to be introduced in the model.

The attraction between solvophobic part of dendrimer and solvophobic compounds increases the amount of solubilized compound significantly for all total bead concentrations. At low total bead concentration, the solvophobic monomer is solubilized in the dendrimer core and the solvent is forced out without significant changes in dendrimer conformations. With increasing total bead concentration, the amount of solubilized monomer is increasing and simultaneously the solvophobic part of dendrimer is expanded and the solvophilic part is pushed away from the dendrimer centre. For even higher concentrations, non-negligible fraction of solvophobic compound condenses on the dendrimer core surface. In the dendrimers with longer spacers, the amount of solubilized monomers is higher; however the general trends are the same.

The monomer condensation is suppressed in the dendrimers with two outer solvophilic generations due to the higher protection of the dendrimer core by the solvophilic segments.

The increase in the size of solvophobic compound enhances its solubility in the dendrimer core. Segments with lower solvophobicity or with lower attraction to the solvophobic core may be used to obtained the same amount of solubilized segments

if they form tetramer. Under the same conditions as monomer solubilization study, the simulated weight distribution functions of aggregation numbers indicate that all tetramers are solubilized in or condensed on the dendrimer core. Simultaneously, two protective solvophilic generations are not sufficient for the suppression of tetramer condensation on the dendrimer core.

It can be conclued, that from the application point of view, the most perspective systems are dendrimers with relatively long spacer and large enough outer solvophilic shell. The solvophobic compounds with attraction to the dendrimer core are more proper than the compounds without the attraction. Simultaneously the oligomer chains promotes solubilization of solvophobic compounds in the dendrimer.

References

[1] Rubinstein M., Colby R. H.: *Polymer Physics*, Oxford University Press, New York (2003).

[2] Binder K.: *Monte Carlo and Molecular Dynamics in Polymer Science*, Oxford University Press, New York (1995).

[3] Frenkel D., Smit B.: *Understanding Molecular Simulation from Algorithms to Applications*, Academic Press, New York (1996).

[4] Metullio L. et al.: *Polyamidoamine (Yet Not PAMAM) Dendrimers as Bioinspired Materials for Drug Delivery: Structure-Activity Relationships by Molecular Simulations*, Biomacromolecules 5, 1371-1378 (2004).

[5] Bosko J. T.: *Universal Behavior of Dendrimer Solutions*, Macromolecules 44, 660–670 (2011).

[6] Gao C., Yan D.: *Hyperbranched Polymers: from Synthesis to Application*, Prog. Polym. Sci. 29, 183–275 (2004).

[7] Nanjwade B. K., Bechra H. M., Derkar G. K., Manvi F. V., Nanjwade V. K.: *Dendrimers: Emerging Polymers for Drug-Delivery Systems*, Eur. J. Pharm. Sci. 38, 185-196 (2009).

[8] Svenson S., Tomalia D. A.: *Dendrimers in Biomedical Applications - Reflections on the Field*, Adv. Drug Deliv. Rev. 64, 102-115 (2012).

[9] Gupta U., Agashe H. B., Asthana A., Jain, N. K.: *Dendrimers: Novel Polymeric Nanoarchitectures for Solubility Enhancement*, Biomacromolecules 7(3), 649-658 (2006).

[10] D'Emanuele A., Attwood D.: *Dendrimer–Drug Interactions*, Adv. Drug Deliv. Rev. 57, 2147-2162 (2005).

[11] Fréchet J. M. J.: *Dendrimers and Other Dendritic Macromolecules: From Building Blocks to Functional Assemblies in Nanoscience and Nanotechnology*, J. Polym. Sci. Part A: Polym. Chem. 41, 3713–3725 (2003).

[12] Boris D., Rubinstein M.: *A Self-Consistent Mean Field Model of a Starburst Dendrimer: Dense Core vs Dense Shell*, Macromolecules 29, 7251-7260 (1996). DOI:10.1021/ma960397k

[13] Ganazzoli F., La Ferla R., Terragni G.: *Conformational Properties and Intrinsic Viscosity of Dendrimers under Excluded-Volume Conditions*, Macromolecules 33, 6611-6620 (2000).

[14] Wawrzynska E., Eisenhaber S., Parzuchowski P., Sikorski A., Zifferer G.: *Monte Carlo Simulation Studies of the Size and Shape of Regular Three Generation Dendrimers*, Macromol. Theory. Simul. 23, 288-299 (2014).

[15] Freire J.J., Rubio A.M.: *Conformational Properties and Rouse Dynamics of Different Dendrimer Molecules*, Polymer 49, 2762-2769 (2008).

[16] Klos J.S., Sommer J.U.: *Simulations of Neutral and Charged Dendrimers in Solvents of Varying Quality*, Macromolecules 46, 3107-3117 (2013).

[17] Lescanec R. L., Muthukumar M.: *Configurational Characteristics and Scaling Behavior of Starburst Molecules: A Computational Study*, Macromolecules 23, 2280–2288 (1990)

[18] Murat M., Grest G.: *Molecular Dynamics Study of Dendrimer Molecules in Solvents of Varying Quality*, Macromolecules 29, 1278–1285 (1996).

[19] Welch P., Muthukumar M.: *Tuning the Density Profile of Dendritic Polyelectrolytes*, Macromolecules 31, 5892-5897 (1998).

[20] Welch P., Muthukumar M.: *Dendrimer−Polyelectrolyte Complexation: A Model Guest−Host System*, Macromolecules 33, 6159-6167 (2000).

[21] Terao T., Nakayama T.: *Molecular Dynamics Study of Dendrimers: Structure and Effective Interaction*, Macromolecules 37, 4686–4694 (2004).

[22] Lyulin S.V., Evers L.J., van der Schoot P., Darinskii A.A., Lyulin A.V., Michels M. A. J.: *Effect of Solvent Quality and Electrostatic Interactions on Size and Structure of Dendrimers. Brownian Dynamics Simulation and Mean-Field Theory*, Macromolecules 37, 3049–3063 (2004).

[23] Efthymiopoulos P., Kosmas M., Vlahos C., Gergidis L. N.: *Conformational Properties of Dendritic Homopolymers with Interacting Branching Points*, Macromolecules 40, 9164-9173 (2007).

[24] Suek N. W., Lamm M. H.: *Effect of Terminal Group Modification on the Solution Properties of Dendrimers: A Molecular Dynamics*, Macromolecules 39, 4247-4255 (2006).

[25] Freire J.J.: *Realistic Numerical Simulations of Dendrimer Molecules*, Soft Matter 4, 2139-2143 (2008).

[26] Martinho N., Florindo H., Silva L., Brocchini S., Zloh M., Barata T.: *Molecular Modeling to Study Dendrimers for Biomedical Applications*, Molecules 19.2, 20424-20467 (2014).

[27] Ma Y., et al.: *Theoretical and Computational Studies of Dendrimers as Delivery Vectors*, Chem. Soc. Rev. 42.2, 705-727 (2013).

[28] Jain V., Bharatam P.V.: *Pharmacoinformatic Approaches to Understand Complexation of Dendrimeric Nanoparticles with Drugs*, Nanoscale 6.5, 2476-2501 (2014).

[29] Lin C.M., Wu Y.F., Tsao H.K., Sheng Y.J.: *Studies of Drug Delivery and Drug Release of Dendrimer by Dissipative Particle Dynamics*, (2008).
In COMPLEX SYSTEMS: 5th International Workshop on Complex Systems Vol. 982, No. 1, pp. 525-527. AIP Publishing.

[30] Hoogerbrugge P. J., Koelman J. M. V. A.: *Simulating Microscopic Hydrodynamic Phenomena with Dissipative Particle Dynamics.*, Europhys. Lett. 19, 155 (1992).

[31] Groot R. D., Warren P. B.: *Dissipative Particle Dynamics: Bridging the Gap between Atomistic and Mesoscopic Simulation*, J. Chem. Phys. 107, 4423-4435 (1997).

[32] Groot R. D.: »Applications of Dissipative Particle Dynamics.« *Novel Methods in Soft Matter Simulations*, Springer Berlin Heidelberg, 5-38 (2004).

[33] Seaton M. A., Smith W.: *DL_MESO User Manual*, STFC Daresbury Laboratory (2012)
`http://www.stfc.ac.uk/CSE/resources/pdf/USRMAN.pdf`.

[34] Seaton M. A., Anderson R. L., Metz S., Smith W.: *DL_MESO: Highly Scalable Mesoscale Simulations*, Molecular Simulation (2013)
`DOI:10.1080/08927022.2013.772297`.

[35] Español P., Warren P. B.: *Statistical Mechanics of Dissipative Particle Dynamics*, Europhys. Lett. 30, 191-196 (1995).

[36] Munk P., Aminabhavi T. M.: *Introduction to Macromolecular Science*, John Wiley & Sons, Inc., New York (2002).

[37] Tanis I., Karatasos K.: *Molecular Dynamics Simulations of Polyamidoamine Dendrimers and Their Complexes with Linear Poly(ethylene oxide) at Different pH Conditions: Static Properties and Hydrogen Bonding*, Phys. Chem. Chem. Phys., 11, 10017-10028 (2009).